AD NUMBER

AD458049

NEW LIMITATION CHANGE

TO

Approved for public release, distribution unlimited

FROM

Distribution authorized to U.S. Gov't. agencies and their contractors; Administrative/Operational Use; Jan 1965. Other requests shall be referred to David Taylor Model Basin, Washington, DC.

AUTHORITY

NSRDC ltr, 7 Oct 1980

DEPARTMENT OF THE NAVY

HYDROMECHANICS

o

AERODYNAMICS

o

STRUCTURAL MECHANICS

o

APPLIED MATHEMATICS

o

ACOUSTICS AND VIBRATION

RESPONSE OF 9M10,000-H RESILIENT MOUNTS UNDER SHOCK LOADING

by

Earl A. Thornton, Robert D. Short, Jr.
and Ramon R. Walker

STRUCTURAL MECHANICS LABORATORY
RESEARCH AND DEVELOPMENT REPORT

January 1965 Report 1899

RESPONSE OF 5M10,000-H RESILIENT MOUNTS UNDER SHOCK LOADING

Earl A. Thornton, Robert D. Short, Jr.
and Ramon R. Walker

January 1965

Report 1899
Special Project

TABLE OF CONTENTS

TABLE OF CONTENTS

LIST OF FIGURES

LIST OF FIGURES (continued)

LIST OF FIGURES (continued)

LIST OF TABLES

GENERAL NOTATION

c	Viscous damping constant
D_0	Snubber clearance
F	Force
i	$= \sqrt{-1}$
k	Spring constants
M	Mass
t	Time
v	Velocity
X	Absolute displacement
Z	Relative displacement

ABSTRACT

Experimental and theoretical studies of the type 5M10,000-H rubber resilient mount assembly consisting of a compression and shear mount and snubber were conducted to determine its performance under shock loading.

In the experimental study, the mount assembly (supporting a rigid test mass) was installed on the Floating Shock Platform and subjected to a series of five shock tests. The experimental data were analyzed and dynamic force-deflection curves were obtained.

Parallel theoretical studies were conducted. A simple mathematical model combining springs and dashpots was used to represent the response of the mounts under vertical shock loading. Theoretical dynamic force-deflection curves obtained from this system showed good agreement with the experimental data.

Findings of the experimental and theoretical studies led to the conclusion that dynamic force-deflection curves must be used in calculations of the shock response of supported equipment.

INTRODUCTION

BACKGROUND

Resilient mounting systems are used to reduce the structureborne noise introduced by machinery items on modern Naval vessels. The resilient mounts are generally made of natural rubber, have relatively low static spring constants, and exhibit natural frequencies at rated loads from about 5 cps to 25 cps. The rated load per mount varies according to size and is from about 15 lb to 10,000 lb. Low mount stiffness permits movement of the supported machinery due to internal vibration, and also permits excursions due to ship maneuvers and attacks from underwater explosions. To limit the excursions to acceptable values, snubbers are used as a component of the mounting system. The snubbers have the functions of:

(1) reducing the requirements for the flexible piping connections that are attached to the machinery;

(2) conserving space by reducing the clearance allowed for excursions of the machinery; and

(3) preventing the machinery from coming adrift under severe shock loadings.

The need for understanding the performance of resilient mount behavior under shock loading has become increasingly important as the shock requirements for Naval ships have increased. Several questions concerning the performance of resilient mounts under higher attack severities have arisen. One of the most

important areas concerns the shock mitigation characteristics of the mounts. In this area the dynamic characteristics of rubber are found to have an important role. It has been established that the stiffness of rubber increases with increasing loading rates.[1]

A number of resiliently mounted items have been shock tested on the Floating Shock Platform (FSP) as a part of the Navy's shock-hardening program. Where possible, the David Taylor Model Basin (DTMB) has studied the performance of these mounting systems to gain insight into the behavior of the mounts under dynamic conditions. In this way, some preliminary information concerning the performance of 5M10,000-H resilient mount assembly was obtained.[2] (The preliminary evaluation is described in Appendix A.) Results of these tests showed that the dynamic behavior of the mounts differs significantly from that based on static tests. However, the study of the data from these tests indicated a need for controlled experiments since extraneous effects introduced by vibrations of the equipment obscured the details of the dynamic behavior of the mounts. To meet this need, a rigid, concentrated mass was designed and constructed for the purpose of evaluating mount behavior; the resiliently mounted mass was tested on the FSP. This report presents the results and analysis of 5M10, 000-H mount shock tests using this test fixture. Tests are planned for 5B5,000-H mounts; results of these tests will be reported separately at a later date.

Analytical studies were conducted to supplement the experimental investigations. The analytical studies established a simple mathematical model to represent the dynamic behavior of the mounts. Future investigation will attempt to establish simple methods of determining the parameters required for the mathematical model and to correlate these parameters with physical characteristics of the resilient mounts.

OBJECTIVES

The overall objectives of the investigation of the behavior of resilient mounts under shock loading are:

(a) establish the performance of existing types of resilient mounts;

(b) determine the important characteristics of resilient mounts for effective shock isolation; and,

(c) develop simplified techniques for predicting the behavior of existing and new designs of resilient mounts.

The specific objectives of the investigation covered by the present report concerned with the shock tests and analysis of 5M10,000-H resilient mounts are:

[1] References are listed on page 39.

(a) determine the response of the mounts during vertical shock loading;

(b) determine the dynamic force-deflection curves;

(c) compare the response of the mounts to static and dynamic loading; and,

(d) develop a simple mathematical model for predicting the action of the mounts under dynamic loading.

SCOPE OF REPORT

Descriptions of the test fixture, the mount installation, the instrumentation used to document the shock environment and the mount behavior, and the tests are given under Test Procedure. Typical instrumentation results and a description of the deformations sustained by the mounts are given under Test Results.

In the analysis of the experimental results that follows, Analysis of the Resilient Mount Response, the loading sequence and the response of the mounts are described first and then a description of the method for determining the dynamic force-deflection curves with the results is presented. This in turn is followed by a Theoretical Analysis of the Resilient Mount Response. Then, under the Discussions of Results, the significance of the effect of dynamic loading is considered and a comparison of dynamic and static force-deflection curves is made. In the last section, general conclusions are drawn.

The report is supplemented by three appendixes. The preliminary evaluation of the mounts based on the FSP tests of a resiliently mounted propulsion turbine is given in Appendix A; static test results are given in Appendix B; and details of the analog computer program are given in Appendix C.

TEST PROCEDURE

INSTALLATION

Tests of resiliently mounted equipment on the FSP had indicated that a rigid, concentrated mass was required for an accurate study of the mount behavior under shock. To fulfill this requirement a mass that consisted of a rectangular steel box filled with lead was constructed. It was a 5-ft-long box with a 2-ft-square cross-section and was fabricated of 1-in.-steel plate. Lead was poured into it to give a total weight of about 16,000 lb. Prior to the pouring of the lead, the inner surfaces of the box were tinned to aid in securing a bond between the two materials.

Eight 1-in. -diameter steel studs were inserted transversely through the lead to clamp the lead between the sides of the box. Two instrumentation pads were permanently imbedded in the top surface of the lead. The weight installed on the FSP is shown in Figure 1.

Figure 1 - General View of the Rigid,Concentrated Mass

The weight was supported on the FSP by two 5M10,000-H resilient mounts. These were installed upon a special foundation fabricated from heavy steel plate welded to the FSP inner bottom.

Each of the 5M10,000-H mounts consists of three components[3]:

(1) a compression mount to support the major portion of the static vertical load;

(2) a shear mount to stabilize the static load with respect to lateral motion and support about 16 percent of the static vertical load; and,

(3) a snubber assembly to limit vertical and lateral excursions under dynamic conditions.

Figure 2 is a photograph of the three components prior to installation. A view of both sets of components installed in the test fixture is in Figure 3. This view shows the upper snubber components located near each end of the weight and the shear and compression components located near the center.

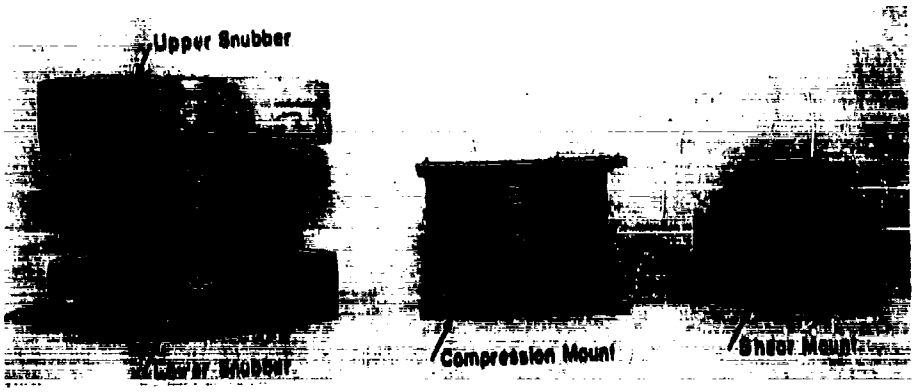

Figure 2 - Components of the 5M10,000-H Resilient Mount

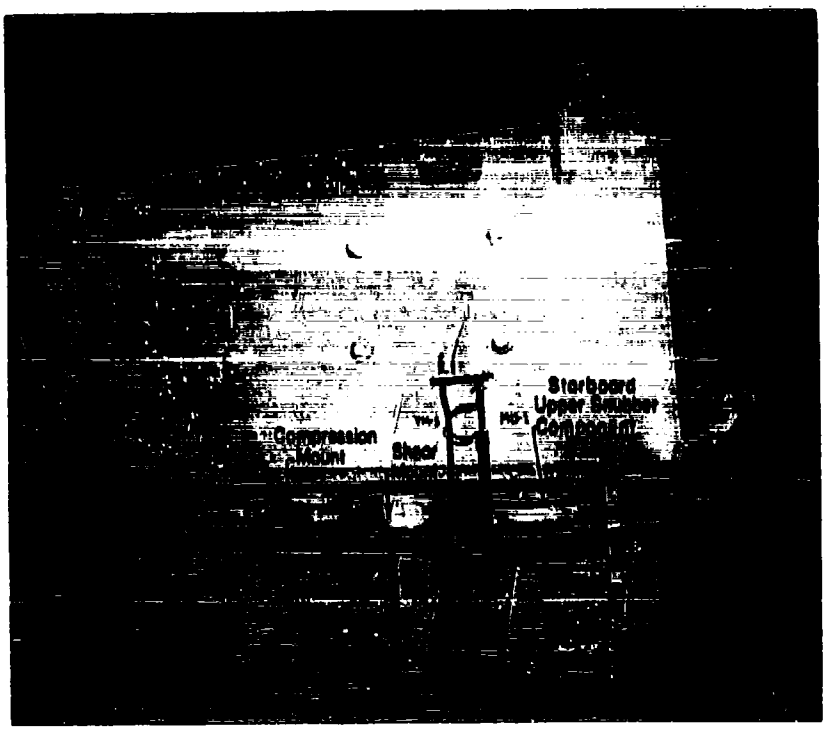

Figure 3 - Mount Components in Completed Test Fixture

The shear and compression components were installed in a symmetrical arrangement to aid in establishing static stability. A clearance was maintained between the upper snubbers and the foundation. A similar clearance was maintained for the lower snubbers, which are hidden in the photograph by the foundation supports. These clearances were set prior to testing at 5/16 in. and 1/8 in., respectively.

INSTRUMENTATION

The inner bottom of the Floating Shock Platform and the test fixture were instrumented with nine velocity meters (VM), six mechanical deflection gauges (MD), and two accelerometers (ACC). The gauges were located to measure the shock input, the relative motion between the weight and foundation, and the absolute motion of the weight. The gauge locations are tabulated in Table 1 and are shown schematically in Figures 4 and 5. Typical installations are shown in Figures 1 and 3. Three high-speed motion picture cameras were used to document the response of the weight and mounts.

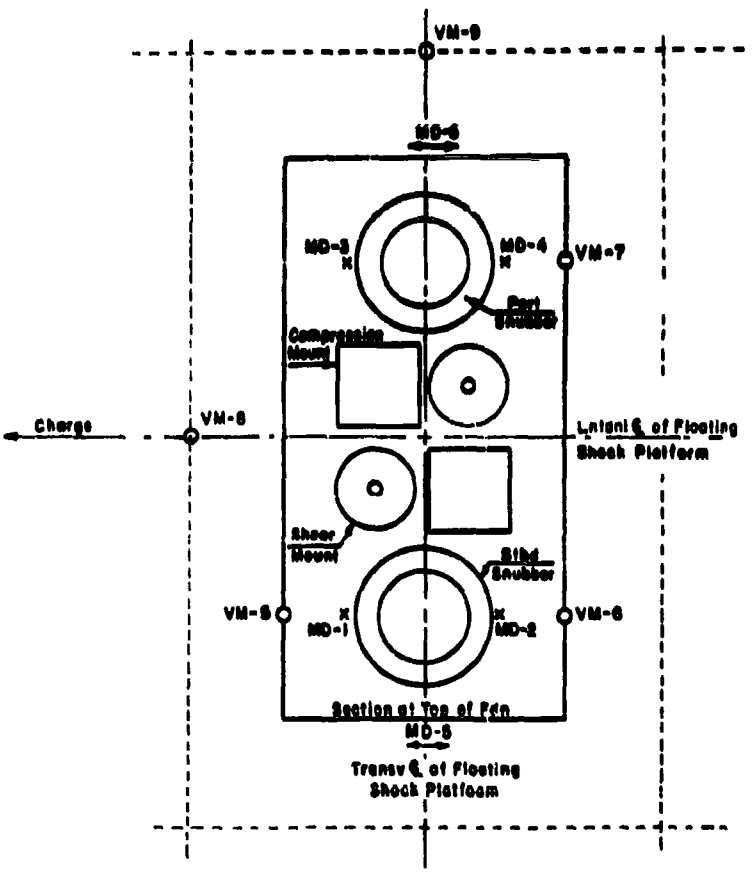

Figure 4 - Instrumentation Schematic - Plan View

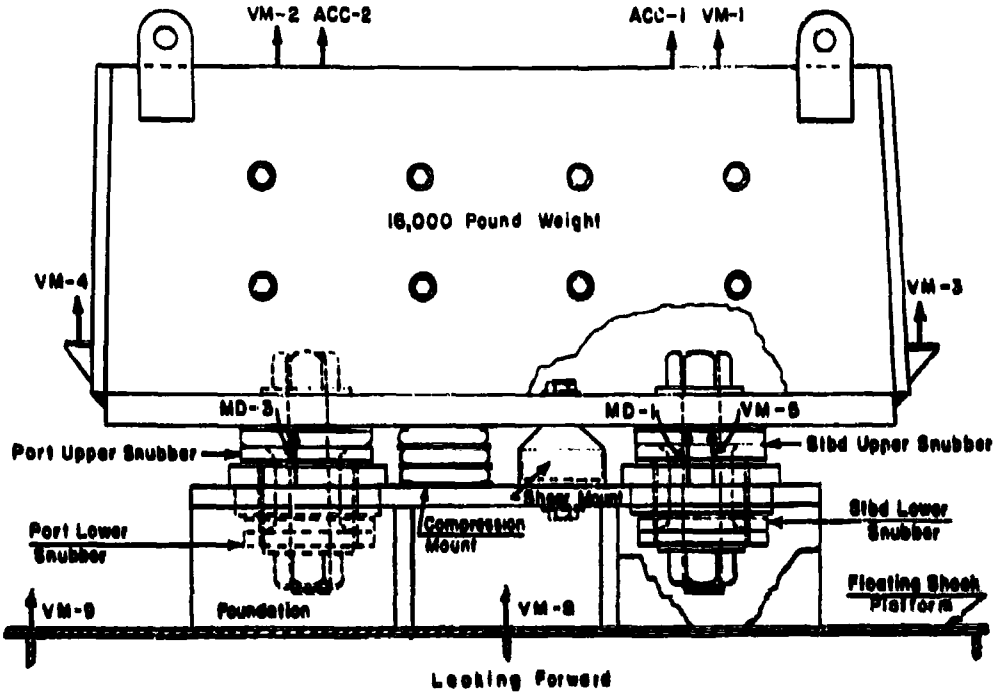

Figure 5 - Instrumentation Schematic - Elevation

TABLE 1
Instrumentation Locations

Gauge	Location	Quantity Measured
VM-1	Top of weight, Centerline of starboard instrumentation pad	Absolute velocity
VM-2	Top of weight, Centerline of port instrumentation pad	Absolute velocity
VM-3	Bottom of weight, Centerline of starboard end of weight	Absolute velocity
VM-4	Bottom of weight, Centerline of port end of weight	Absolute velocity
VM-5	Bottom of weight to foundation, starboard snubber, aft side	Relative velocity
VM-6	Bottom of weight to foundation, starboard snubber, forward side	Relative velocity
VM-7	Bottom of weight to foundation, port snubber, forward side	Relative velocity
VM-8	Floating shock platform deck, amidships, aft side	Absolute velocity
VM-9	Floating shock platform deck, port end of weight on centerline	Absolute velocity
ACC-1	Top of weight, Centerline of starboard instrumentation pad	Absolute acceleration
ACC-2	Top of weight, Centerline of port instrumentation pad	Absolute acceleration
MD-1	Bottom of weight to foundation, starboard snubber, aft side	Relative vertical displacement
MD-2	Bottom of weight to foundation, starboard snubber, forward side	Relative vertical displacement
MD-3	Bottom of weight to foundation, port snubber, aft side	Relative vertical displacement
MD-4	Bottom of weight to foundation, port snubber, forward side	Relative vertical displacement
MD-5	Bottom of weight to foundation, starboard side	Relative horizontal displacement
MD-6	Bottom of weight to foundation, port side	Relative horizontal displacement

TESTING

Static compression tests of the resilient mounts were conducted prior to the installation of the test fixture in the FSP. The results of these tests are presented in Appendix B.

Five underwater explosion tests of increasing severity were conducted. A tabulation of the test data is given in Table 2.

TABLE 2
Test Data

Test No.	Standoff	Charge Depth	Charge Weight-TNT
	ft	ft	lb
1	65	24	87
2	40	24	87
3	30	24	87
4	20	24	87
5	20	20	130.5

A schematic of the test geometry is given in Figure 6. It should be observed that the charge was located opposite the after end of the FSP.

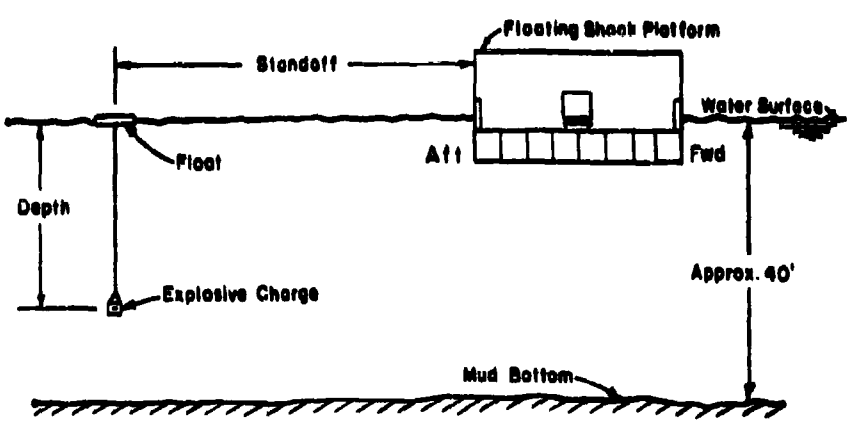

Figure 6 Schematic of Test Geometry

TEST RESULTS

SHOCK ENVIRONMENT

The shock environment of the FSP resembles the shock motions experienced by the double bottom of a surface ship. Typical velocity histories for the FSP indicate that the motion is essentially vertical. This vertical motion is characterized by a large initial acceleration rapidly reaching a peak velocity that is followed by a deceleration phase of much longer duration. This motion is followed by a reloading phase which introduces a lower level of acceleration. Input motions of this type were recorded by VM-8 and VM-9. These meters show similar results except that VM-8 showed slightly larger magnitudes since it was closer to the charge. VM-9, however, should be more representative of the shock input to the test fixture. A typical history recorded by this meter is shown in Figure 7.* Peak velocities and the corresponding shock factor for this location are given in Table 3 for each test.

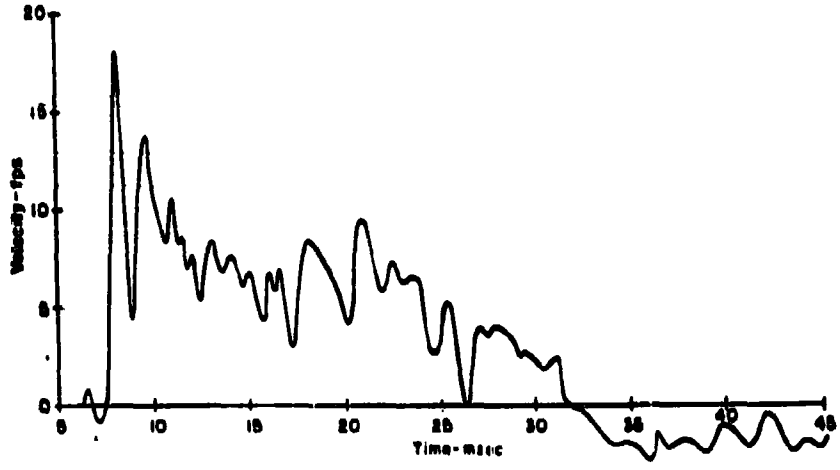

Figure 7 - Typical Input to the Foundation

TABLE 3
Shock Input Data

Test No.	Shock Factor*	Peak Velocity (fps)
1	0.07	4
2	0.11	6.5
3	0.14	8.5
4	0.18	12
5	0.23	16

*Shock Factor = $\frac{\sqrt{W}}{R}\ \frac{1+\sin\theta}{2}$ where W is the charge weight in pounds of TNT, R is the slant range, and θ is the angle between R and the horizontal.

*In this figure as well as in Figures 9, 10 and 11 that follow, zero time corresponds to detonation of the charge.

RESPONSE OF MASS

The response of the mass was documented by a number of meters that were selected to record the absolute velocity and acceleration of the mass and the relative displacement between the mass and foundation. The velocity and acceleration data were important to determine the forces transmitted by the mounts, and the deflections to indicate the deformations experienced.

Except for the first test, these measurements indicate that the snubbers of each mount engaged during the response of the mass. For the first test, the measurements and the motion pictures indicate that only one snubber engaged as the result of rocking motions of the mass introduced by rolling of the FSP prior to charge detonation. Because of these rocking motions, the clearances of each snubber were significantly different at the instant of shock loading. To eliminate this complication, on subsequent tests small steel brackets were welded between the foundation and bottom of the mass to maintain the desired snubber clearances. These brackets were deformed laterally prior to installation so that during the early phases of shock loading, buckling failures of the brackets did occur. Two of these brackets prior to testing are visible in Figure 8.

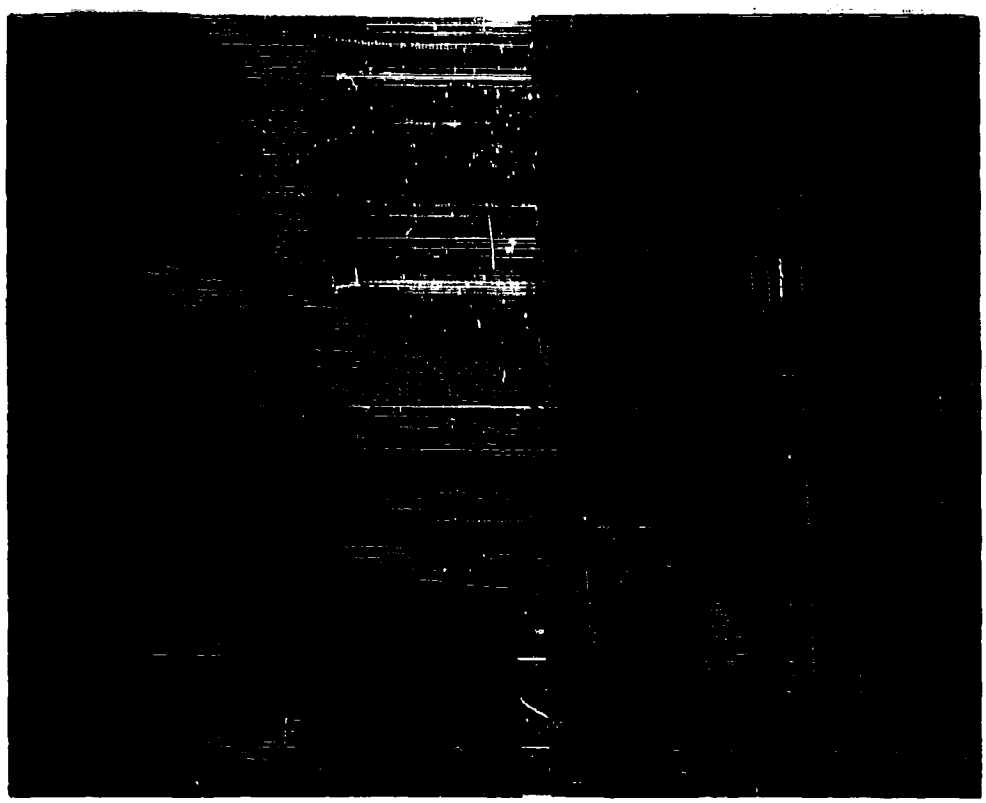

Figure 8 - Static Support Brackets

The motion of the mass during the last four tests clearly indicates that both snubbers engage. This fact is evident from the deflection gauges, but is more clearly demonstrated by the periods of sharp acceleration shown by the records of velocity meters and accelerometers mounted on the mass. A typical velocity history of the mass recorded by VM-1 is given in Figure 9. A typical acceleration history is given in Figure 10.

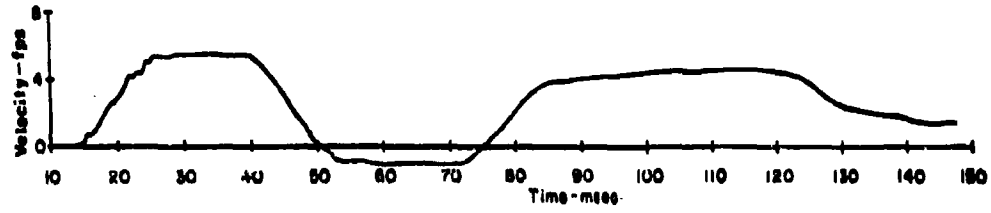

Figure 9 - Typical Velocity History of Mass

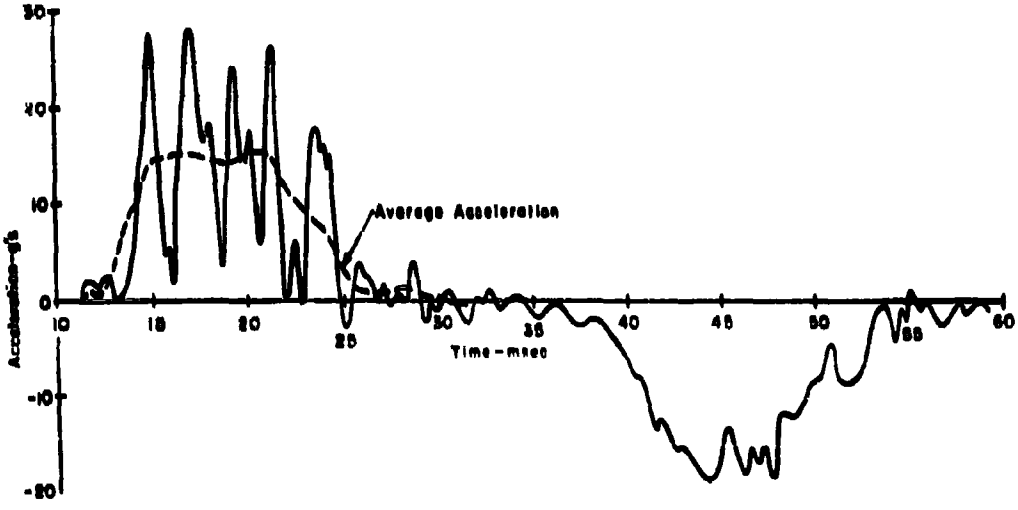

Figure 10 - Typical Acceleration History of Mass

An examination of the deflection gauges for each test indicates that for the last four tests the mass responded as a vertical translation without port to starboard rotation. These records show that both port and starboard snubbers engage simultaneously. The deflection gauges indicate that a rocking motion occurs in the forward-aft direction. This motion has a low frequency and is not pronounced during the initial loading. For this reason it is reasonable to use the average of the forward and aft gauges to represent the vertical translation of the mass. Two typical deflection histories and the average history are given in Figure 11.

The vertical translation of the mass was accompanied by a horizontal motion of a lesser magnitude. During the first compression cycle of the upper snubber,

this translation was about 0.2 in. for most tests. At later times during the response, larger horizontal deflections occurred up to a maximum of about 0.4 inch.

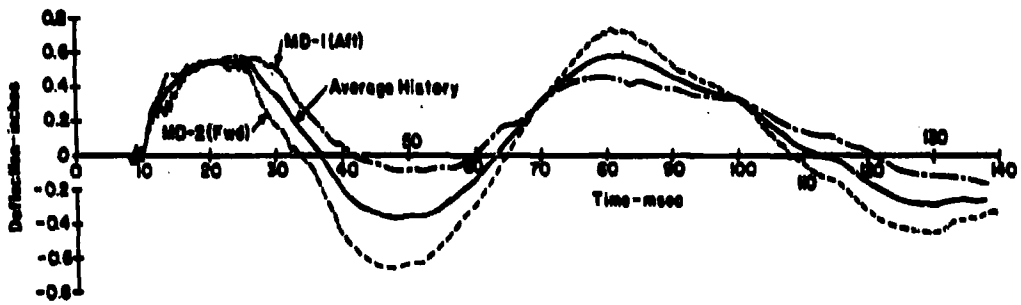

Figure 11 - Typical Vertical Deflection Histories

RESILIENT MOUNT DEFORMATION

The rubber portions of the resilient mount components underwent considerable deformation during the shock response. The extent of the deformations is clearly seen in the high-speed motion pictures. The sequence of events and the extent of the deformation for the most severe test may be seen in Figure 12. In this figure, photographs obtained from one of the motion picture films are given for significant times during the first loading of the upper snubber.

The first photograph shows the upper snubber at the time of charge detonation. In the second one, the snubber clearance has closed and the snubber is about to engage. The next two show the snubber deformation, as the maximum displacement is reached. The fifth one shows the snubber deformation during the unloading phase, and the last one shows the snubber slightly after separation occurs. The deformation of the rubber at this time is clearly visible.

Permanent damage sustained by the mounts as a result of the shock loadings was relatively minor. The one significant case of damage proved to be a crack that developed between the bonding surface of metal and rubber on one of the snubbers. This damage, however, did not appear to have any serious detrimental effects since static load-deflection curves obtained before and after the shock tests show good agreement.

In this section, the important aspects of the shock input and the response of the mass have been described. In the next section these results are interpreted in terms of the mount behavior and dynamic force-deflection curves for the mounts are derived.

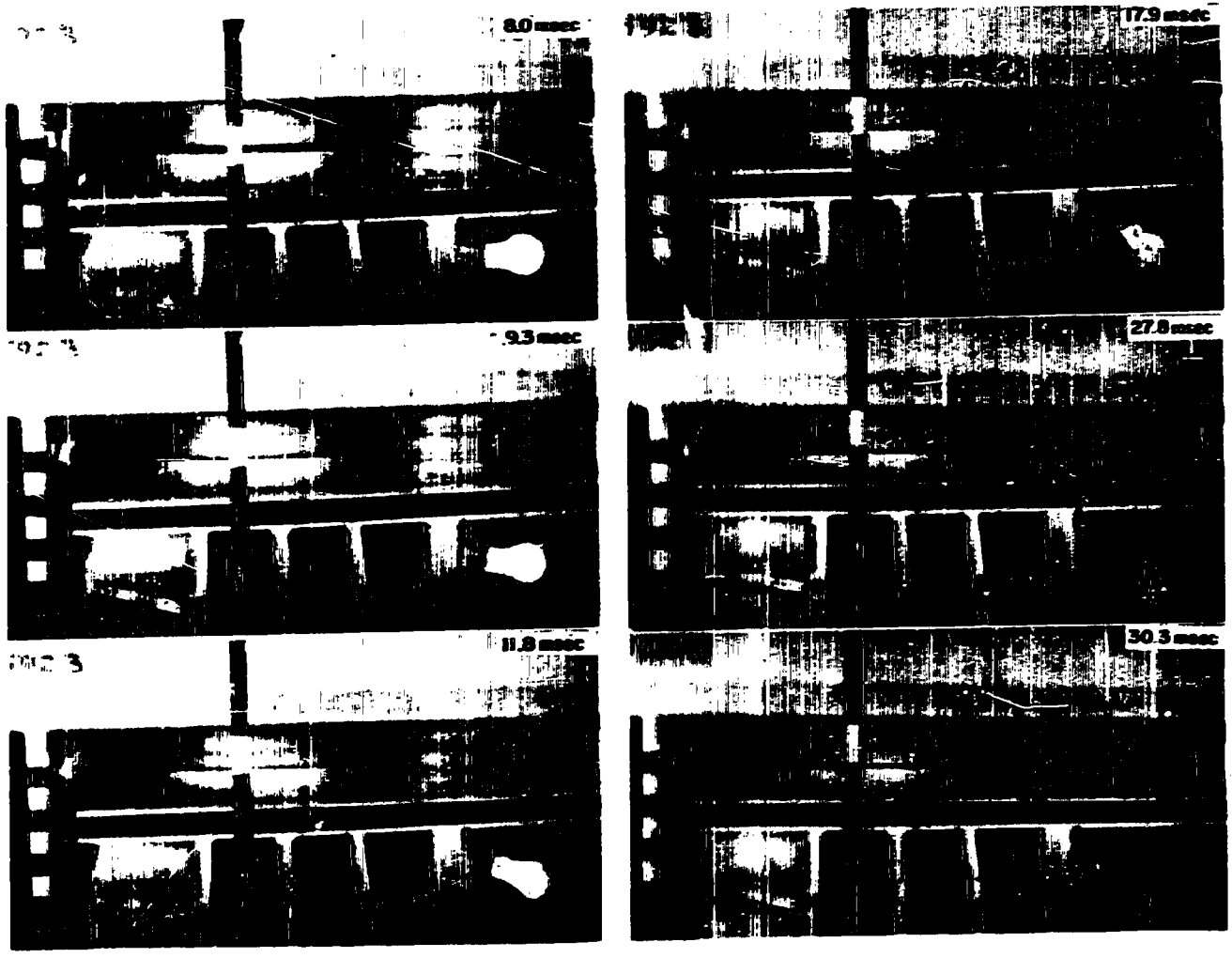

Figure 12- Photographs of Mount Response under Shock

ANALYSIS OF THE RESILIENT MOUNT RESPONSE

LOADING SEQUENCE

Examination of the instrumentation histories has indicated that the shock response of the mass consisted essentially of a vertical translation. Although a rocking motion of the mass was present, it was found that for the early portion of the response the loading history of the resilient mountings could be considered in terms of the average displacement of the forward and aft deflection gauges.

For the shock input of the present tests the loading sequence of the 5M10,000-H resilient mounts may be described as follows:

(1) Until the relative vertical displacement between the snubber and foundation decreases by the 5/16-in. original clearance, only the shear and compression mounts exert vertical forces on the mass. During this time, the mass undergoes a small vertical acceleration; however, this acceleration history was not clearly documented by either the velocity histories or the acceleration measurements.

(2) At the time the relative displacement has decreased by the 5/16-in. clearance, the upper snubber engages and the mass subsequently begins to acquire vertical velocity rapidly. After the upper snubber comes into contact the acceleration becomes prominent. This was clearly evident from both the accelerometer records and the velocity histories.

(3) The upper snubber continues to be compressed until the maximum relative displacement is reached. This maximum relative displacement in the present tests varies with the attack severity from about 0.45 to about 0.84 inch. Between the time of snubber engagement and the time of maximum relative displacement the snubber continues to accelerate the mass. During this interval, the acceleration reaches a maximum and begins to decrease before the maximum displacement is reached. This characteristic was demonstrated by both the accelerometer and velocity histories.

(4) After the maximum relative displacement is reached the upper snubber begins to expand. This continues as the relative displacement returns to the original 5/16-in. clearance. However, the force exerted by the snubber does not continue until the 5/16-in. displacement is reached. The test results show that the snubber force reaches zero before this time. For the last test, this fact may be concluded from the photographs (See the last photograph of Figure 12) since the rubber had not returned to its original shape when a clearance opened between the snubber and the foundation.

(5) Following the disengagement of the upper snubber, the relative displacement continues to increase. During this time, the mass is acted upon only by the forces exerted by the shear and compression mounts. The velocity histories showed that the mass moves with almost constant velocity. When the relative displacement has increased to 1/8 in., the lower snubber engages. Beginning at this time, the mass experiences a deceleration and a corresponding decrease in velocity occurs.

(6) The mass experiences the engagement of the upper and lower snubbers on two consecutive cycles. For each of the last four tests, these four engagements were clearly shown on the velocity histories by a sharp acceleration or deceleration of the mass.

DYNAMIC FORCE-DEFLECTION CURVES

The relationships between the dynamic forces transmitted by the mounts and the accompanying deflections are of basic interest in the design of new, more effective, resilient mounting systems. In addition, these results are necessary for the dynamic analysis of equipment supported by systems using resilient mounts of the present types.

To meet this need, dynamic force-deflection curves have been derived from the data of the current tests (Figures 13 through 16).

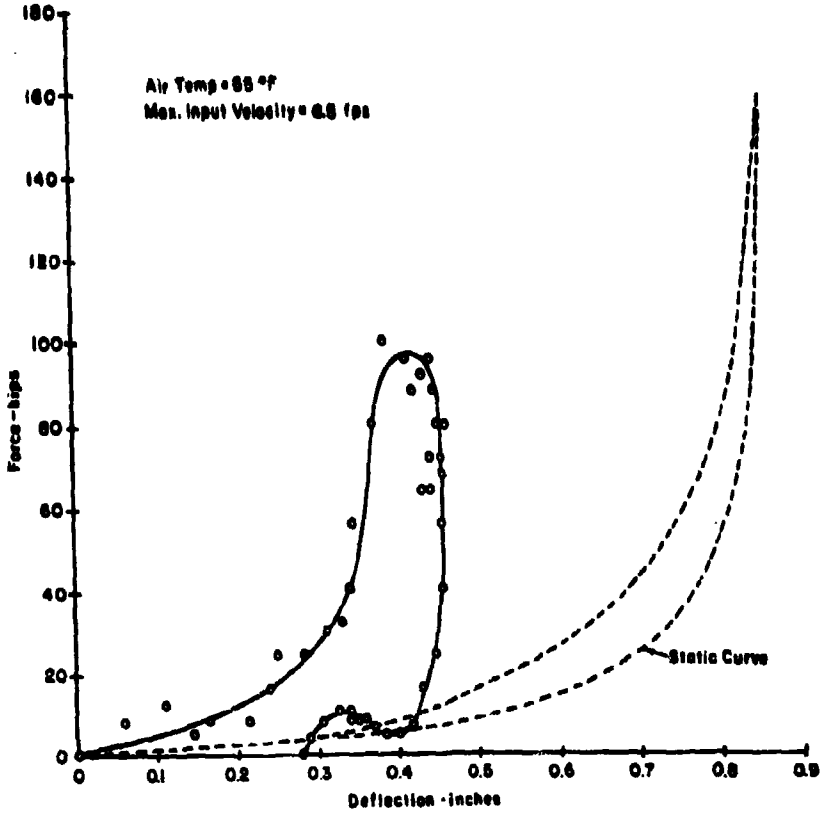

Figure 13 - Dynamic Force versus Deflection - Test 2

The curves were developed for the first compression and expansion of the mount as described above.* Because only one snubber engaged during Test 1, this data was not considered: force-deflection curves were found for Tests 2 through 5.

The dynamic force-deflection curves were found by calculating the instantaneous force transmitted by the mounts from the acceleration histories of the mass. A typical acceleration history of this motion was shown in Figure 10. Typical records, such as this, have indicated that the action of the resilient mount produced an acceleration pulse roughly sinusoidal in shape. Superimposed on each of these pulses were vibrations of higher frequencies.

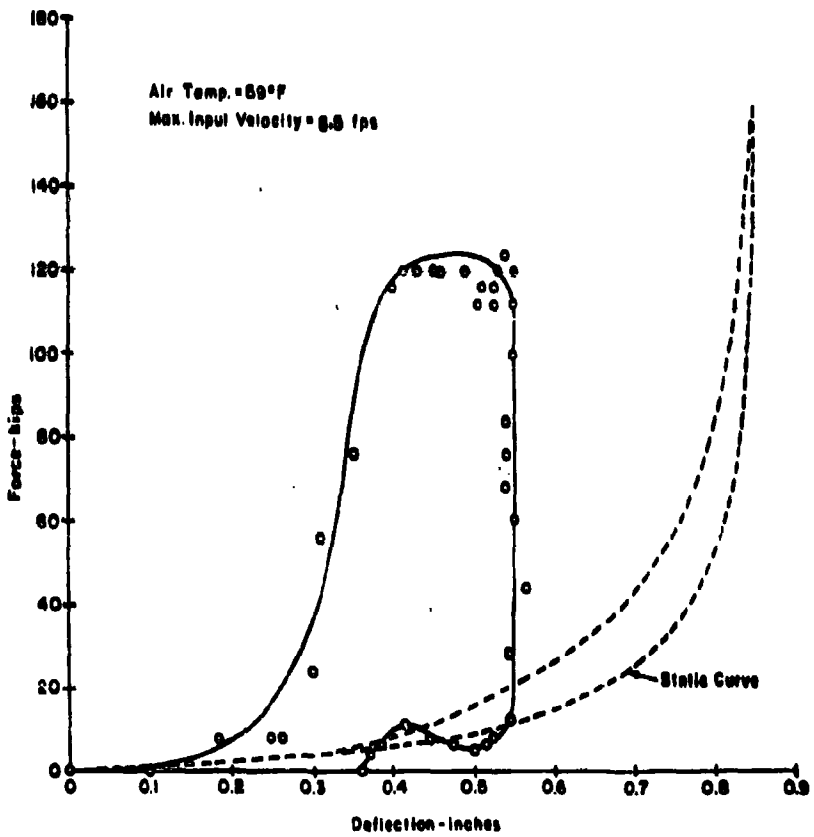

Figure 14 - Dynamic Force versus Deflection - Test 3

*These figures also show the static force-deflection curves from Appendix B.

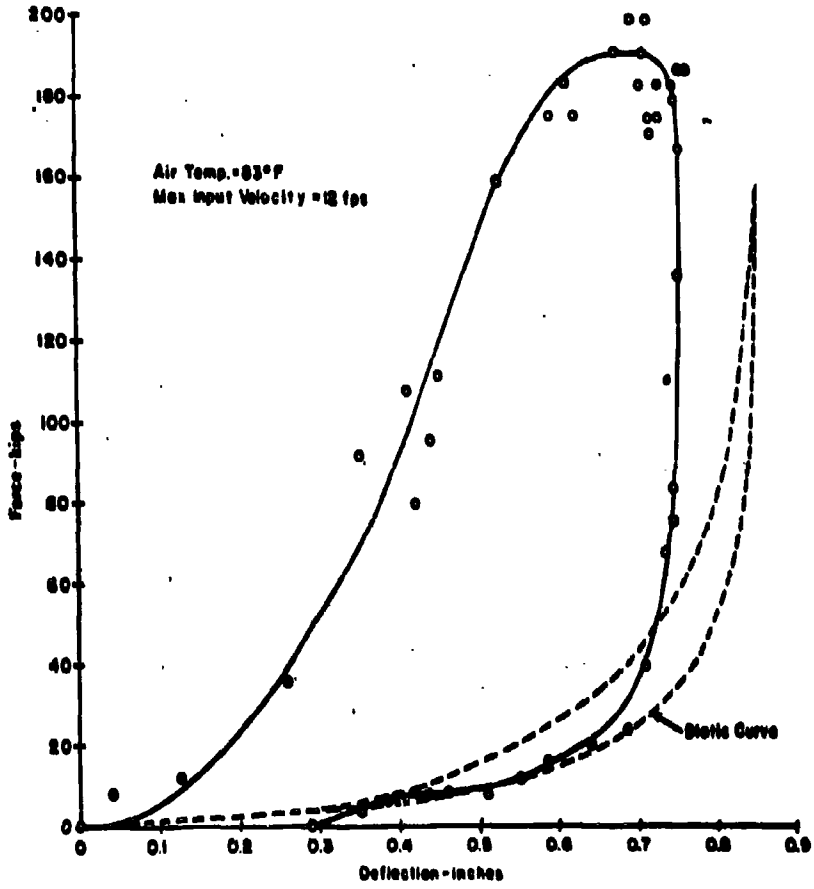

Figure 15 - Dynamic Force versus Deflection - Test 4

These vibrations represent motions other than the rigid body motion of the mass, possibly vibrations of the steel box or the contained lead. To obtain the rigid body acceleration histories of the mass, these vibrations were removed from each record by using an average curve through the center of each superimposed high frequency oscillation. The force transmitted by each resilient mount was then calculated as one-half the supported mass times the instantaneous rigid-body acceleration. Values for forces were calculated in this way at one-half-millisecond intervals. The corresponding mount deflection was read from the average deflection history such as shown in Figure 11.

In this section of the report, the response of the mount under vertical shock loading has been described and dynamic force-deflection curves for the mounts have been derived. These results are discussed and the dynamic and static load-deflection curves are compared in a later section.

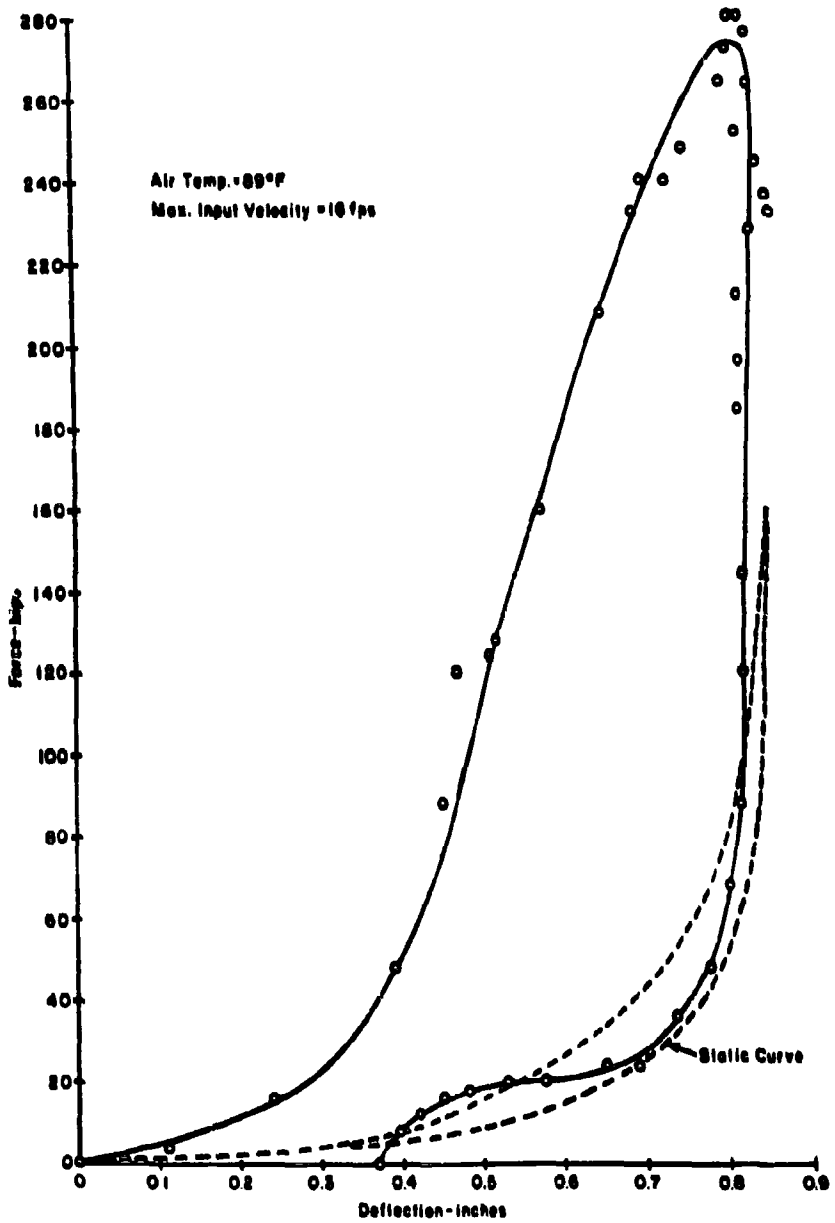

Figure 16 - Dynamic Force versus Deflection - Test 5

THEORETICAL ANALYSIS OF THE RESILIENT MOUNT RESPONSE

GENERAL DEVELOPMENT

The mechanics of deformation of rubber are peculiarly different from the linear, elastic behavior of metallic structures to which most naval architects and marine engineers are accustomed. For the present analysis it is sufficient to observe that under a slowly applied uniaxial load, rubber deforms with a very low elastic modulus (on the order of 10^4 psi) to large strains and with a significant viscosity, all of which are temperature dependent. Under this type of loading, rubber is practically incompressible, and the force-deflection curve is nonlinear, particularly under large loads. On the other extreme, if rubber is constrained so that compressible deformation must occur under a slowly applied load, then the rubber will behave like a true solid with a relatively high modulus of elasticity (on the order of 10^6 psi) and low viscosity and undergo small strains.[4]

One of the distinguishing characteristics of the behavior of rubber under rapidly applied loads is that compressive behavior may play an important role in the response provided the rubber is loaded in such a way that both compressive and shear stresses exist. This behavior occurs as a result of the prominent role of the viscous effects under high rates of deformation. This important role of viscosity has led a number of writers to represent the behavior of the rubber by mathematical models using various combinations of springs and dashpots. One attempt has made use of the Kelvin model.[4] In this case it was found that the material constants were very much dependent on frequency and temperature. The Kelvin model (a spring and dashpot in parallel), however, essentially ignores the compressible features of rubber under high rates of deformation.

The purpose of this section is to present a method of analysing rubber mounts under large dynamic loads which will consider both the compressible properties as well as the usual incompressible properties. For this analysis it is assumed that the loading will have a very short duration (e. g. during an explosion) so that the incompressible deformation will be small, due to the viscosity, and nonlinearities do not have to be considered. A number of mechanical models could be used to represent this behavior. In the present analysis the model shown in Figure 17 will be used. In this system, the upper spring and dashpot represent the incompressible properties while the lower spring represents the compressible property. A mathematically equivalent model known as the "standard linear solid" could have been used to give the same results.[5]

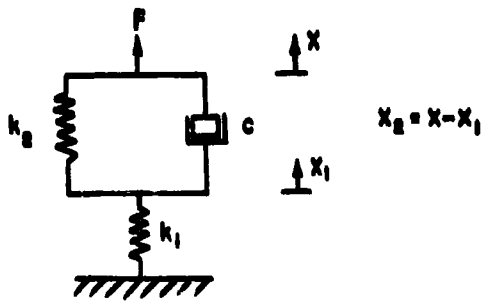

Figure 17 - Mathematical Model of Resilient Mount

The equation of motion for a single-degree-of-freedom system supported by this mount is determined in the following manner. The force-deflection equation for the model of Figure 17 is

$$F = k_1 X_1 = k_2 X_2 + c\dot{X}_2$$

which can be expressed as

$$F = k_1 X - \frac{k_1^2}{c} \exp\left(\frac{-k_1 + k_2}{c} t\right) \int_0^t \exp\left(\frac{k_1 + k_2}{c} \tau\right) X d\tau. \qquad (1)$$

If a mass M is attached to the system, the differential equation describing free vibrations is

$$M\ddot{X} + M\frac{k_1+k_2}{c}\ddot{X} + k_1\dot{X} + \frac{k_1 k_2}{c} X = 0. \qquad (2)$$

If the system is under forced vibration by motion of the base, X_B, then X of Equation 2 is the relative motion, Z. The total motion of the mass, X_t, is then given by

$$M\ddot{X} + \frac{M(k_1+k_2)}{c}\ddot{X} + k_1\dot{X} + \frac{k_1 k_2}{c} X = \frac{k_1 k_2}{c} X_B + k_1 \dot{X}_B. \qquad (3)$$

Since all of the coefficients of Equation (3) are positive, we have from Descartes' rule that the roots of the characteristic equation are either all negative or one is negative and two are complex. Solutions of Equation (3) are all of the form

$$X_n = A_n \exp\left\{-\frac{k_1+k_2}{3c} + \left[\frac{k_1}{M} - 3\left(\frac{k_1+k_2}{3c}\right)^2\right]^{1/2} \frac{n_1}{\sqrt{3}}\right\} t = A_n \exp\{m_n t\} \qquad (4)$$

for n = 1, 2, 3

where

$$\begin{pmatrix} r_1 \\ r_2 \\ r_3 \end{pmatrix} = \left(-\frac{B}{2} + \sqrt{\frac{B^2}{4} + 1}\right)^{1/3} \begin{pmatrix} 1 \\ \exp\left\{\frac{2\pi i}{3}\right\} \\ \exp\left\{\frac{4\pi i}{3}\right\} \end{pmatrix} + \left(-\frac{B}{2} - \sqrt{\frac{B^2}{4} + 1}\right)^{1/3} \begin{pmatrix} 1 \\ \exp\left\{\frac{4\pi i}{3}\right\} \\ \exp\left\{\frac{2\pi i}{3}\right\} \end{pmatrix} \qquad (5)$$

and

$$B = 3\sqrt{3}\left\{\frac{k_1}{M}\left(\frac{2k_2 - k_1}{3c}\right) + 2\left(\frac{k_1 + k_2}{3c}\right)^3\right\}\left\{\frac{k_1}{M} - 3\left(\frac{k_1 + k_2}{3c}\right)^2\right\}^{-\frac{3}{2}} \qquad (6)$$

The general solution of Equation (3) is

$$X = A_1 e^{m_1 t} + A_2 e^{m_2 t} + A_3 e^{m_3 t} + \frac{1}{m_1^2(m_3 - m_2) + m_2^2(m_1 - m_3) + m_3^2(m_2 - m_1)} \int_0^t$$

$$\left[(m_3 - m_2)\, e^{m_1(t-\tau)} + (m_1 - m_3) e^{m_2(t-\tau)} + (m_2 - m_1) e^{m_3(t-\tau)}\right]\left(\frac{k_1 k_2}{Mc} X_B + k_1 \dot{X}_B\right) d\tau. \qquad (7)$$

If the initial conditions, $X(o)$, $\dot{X}(o)$, and $\ddot{X}(o)$ are all zero, then A_1, A_2 and A_3 of Equation (7) are also zero.

5M10,000-H RESILIENT MOUNT RESPONSE PREDICTION

A 5M10,000-H mount under vertical loads may be represented by two parallel systems similar to those of Figure 17, one for the compression and shear mounts and one for the snubber. The shear mount may be considered as a part of the compression mount since its portion of the total load is small. The snubber system will, of course, have a clearance, D_0, under static conditions so that it will not engage until the relative deflection has decreased by this amount. The complete representation for the upper snubber of one mount for vertical loading is shown in Figure 18. A similar mathematical model would also be used to represent the lower snubber. However, the experimental evidence has shown that the initial engagement of the upper snubber gives the largest forces under the present attacks; hence, only the upper snubber will be considered.

The values of k_3 and k_4 were determined from a linear approximation to the static force-deflection curves of Appendix A. This is permissible although k_3 and k_4 are in series with k_1 and k_2, respectively, since the latter are of an order of magnitude larger and are essentially inoperative under static load. The other quantities are essentially dynamic quantities and hence had to be obtained from the experimental test results. Test 4 was selected for this purpose. The system of Figure 18 was programmed on an analog computer (Appendix C) using an analytical representation of the average of the measurements from VM-8 and VM-9 for X_B and the measured spacing for D_0. The quantities k_1, k_2, c_1, and c_2 were then adjusted to obtain the best fit for the measured acceleration, velocity and displacement of the mass up to the time of the first zero of the force (about 20 msec). The values of these constants are given in Table 4. A nonlinear spring closely representing the static curve was also tried for k_4, however, no change was observed in the results. In fact, complete elimination of the spring represented by k_4 resulted in no changes in peak force or deflection and only a very slight alteration to the output. The most noticeable was a one-half millisecond variation in time of snubber separation. Elimination of the spring represented by k_3 also had no effect on the results. However, both k_3 and k_4 were retained as linear springs for the analysis.

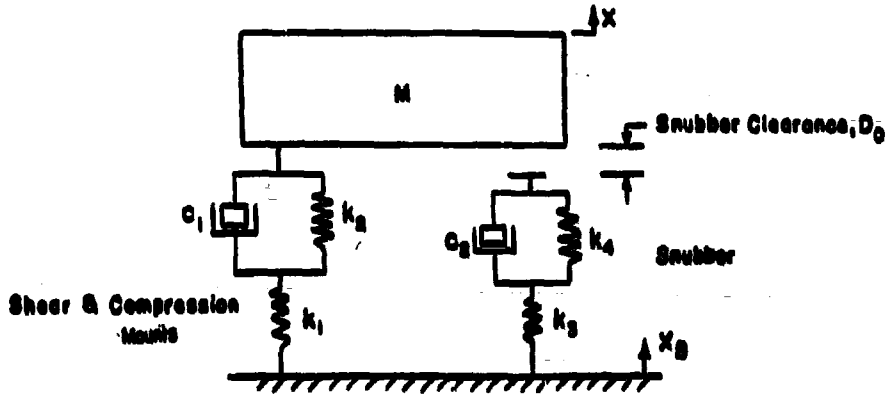

Figure 18 - Mathematical Model of 5M10,000-H Resilient Mount

TABLE 4
Constants for System of Figure 18

k_2 = 62 (kip/in.)	k_3 = 10 (kip/in.)	c_1 = 1.8 (kip-sec/in.)
k_3 = 756 (kip/in.)	k_4 = 40 (kip/in.)	c_2 = 4.71 (kip-sec/in.)
M = 2.5 (slug)	D_0 = 5/16 (in.)	

This system was then applied to Tests 2, 3 and 8. An analytical representation of the average of VM-8 and VM-9 was used for X_B. The analytical representations are shown together with the averaged experimental histories in Figures 19 through 22. *

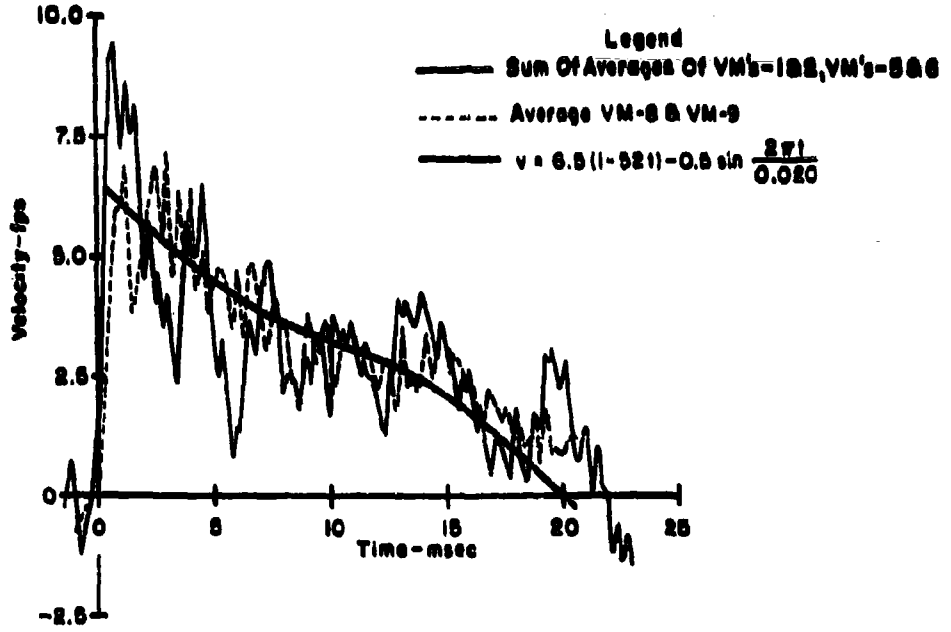

Figure 19 - Average Base Velocity Histories - Test 2

* In these figures as well as Figures 23 through 34, zero time corresponds to the time when the inner bottom motion of the PSP begins.

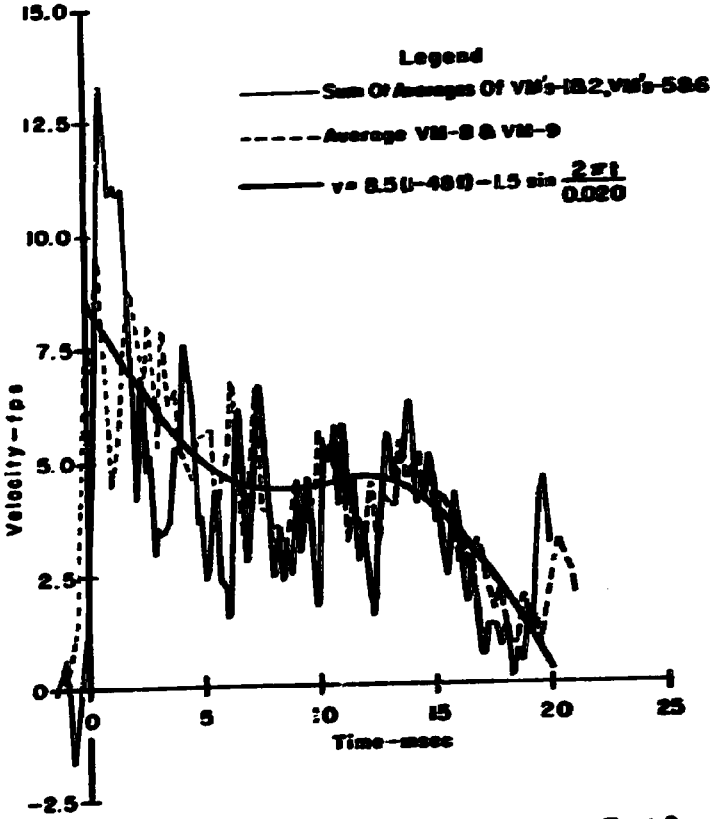

Figure 20 - Average Base Velocity Histories - Test 3

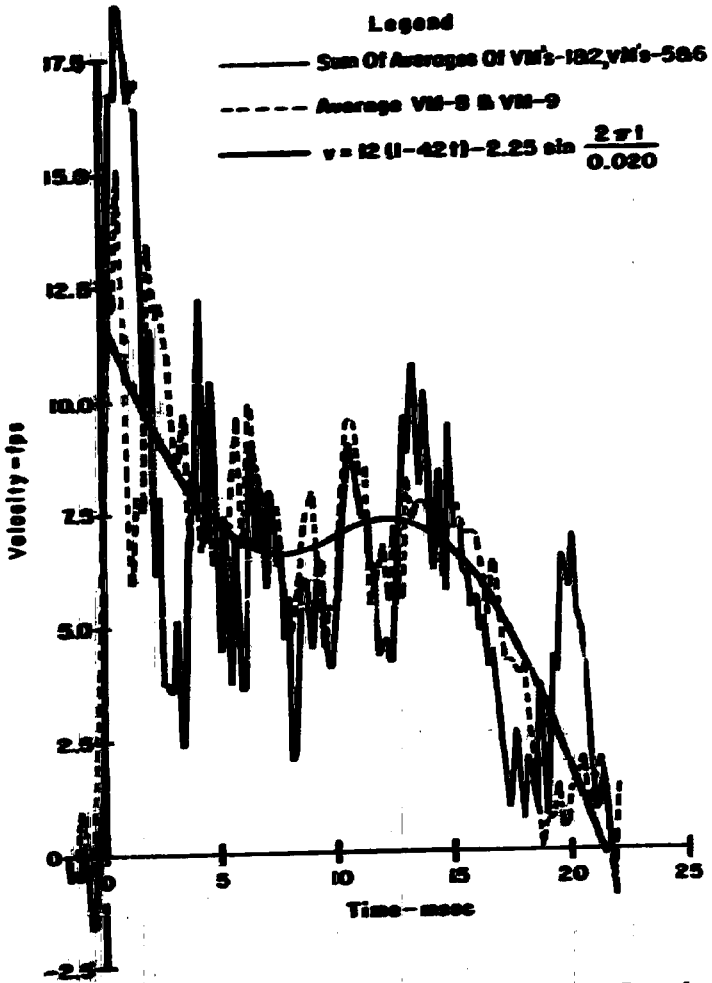

Figure 21 - Average Base Velocity Histories - Test 4

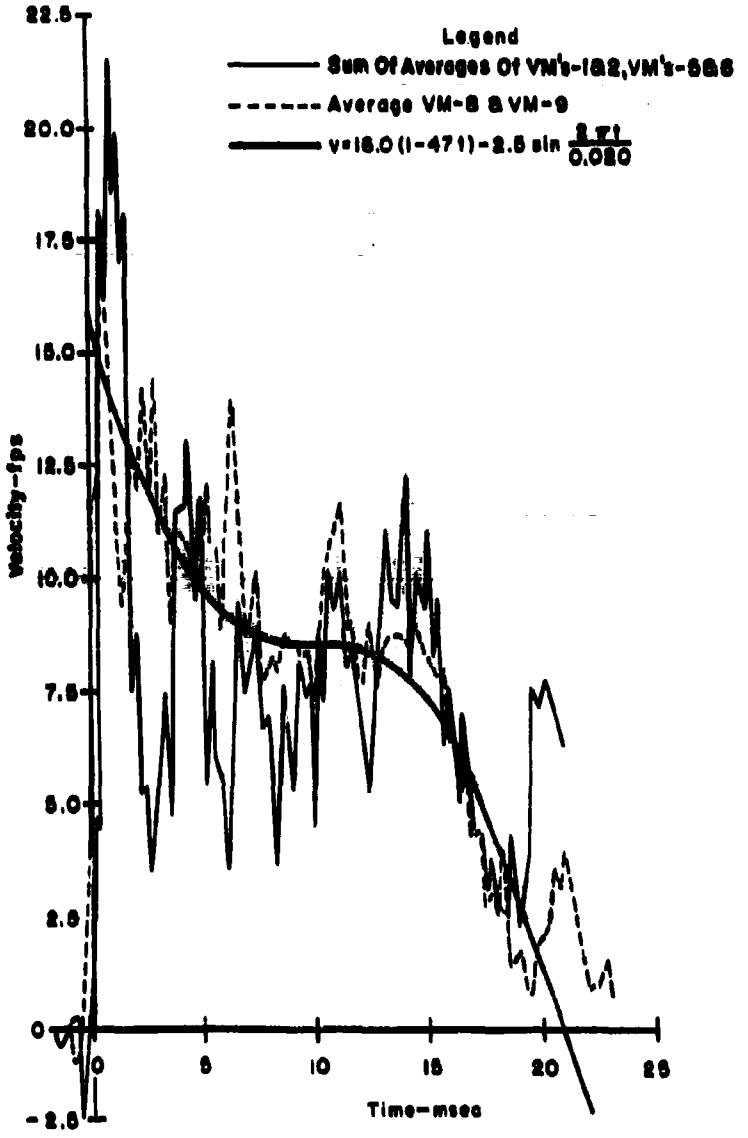

Figure 22 - Average Base Velocity Histories - Test 5

The analog computer solutions for the velocity and relative displacement of the mass and the force-time histories are shown superimposed on the experimental results in Figures 23 through 34. The computed force-deflection curves for each test are shown with the experimental data in Figures 35 through 38.

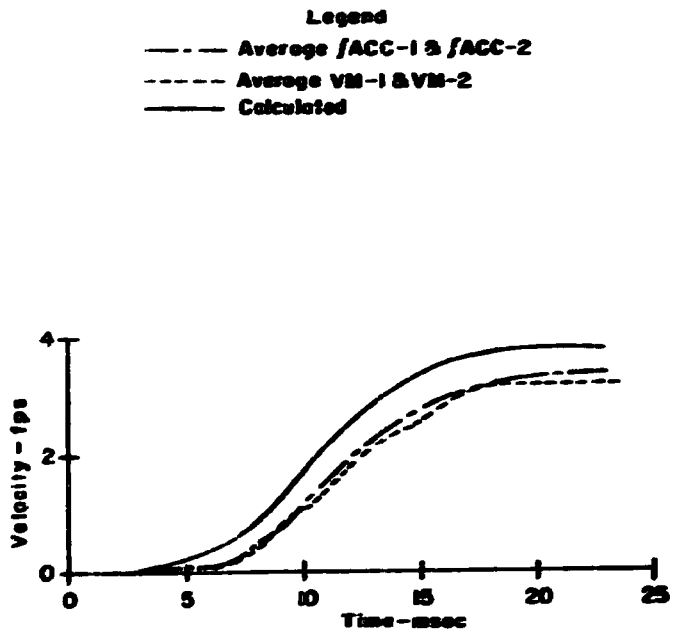

Figure 23 - Velocity Histories of Mass - Test 2

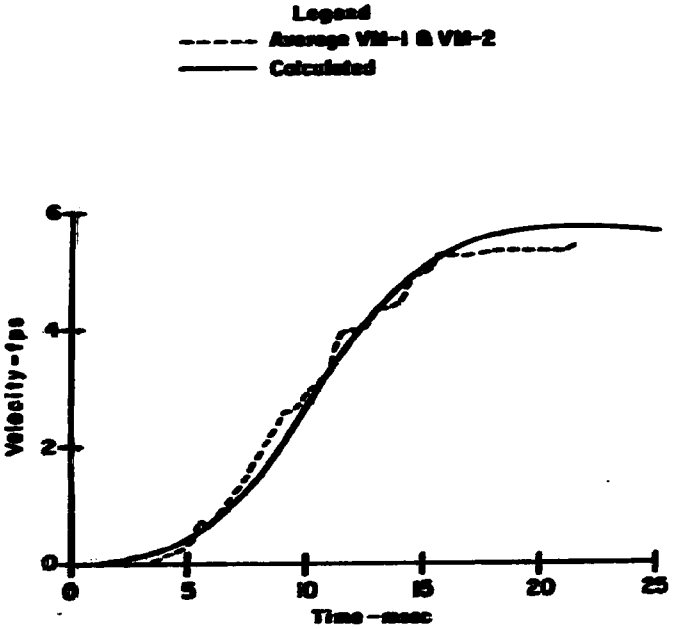

Figure 24 - Velocity Histories of Mass - Test 3

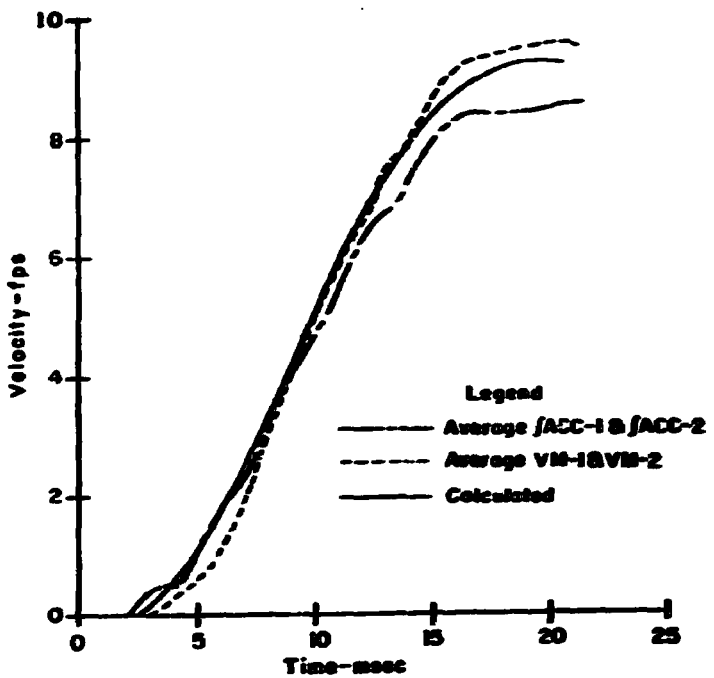

Figure 25 - Velocity Histories of Mass - Test 4

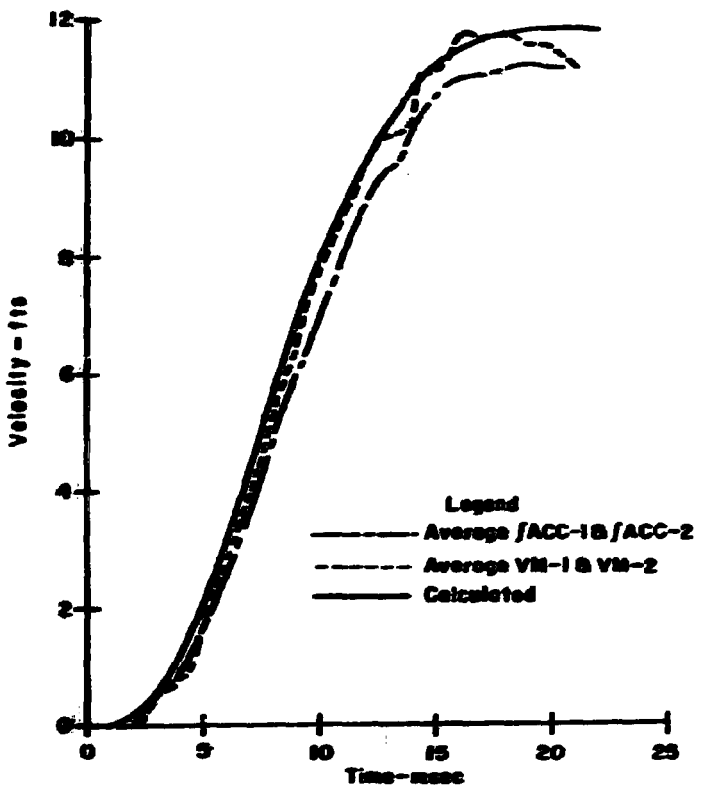

Figure 26 - Velocity Histories of Mass - Test 5

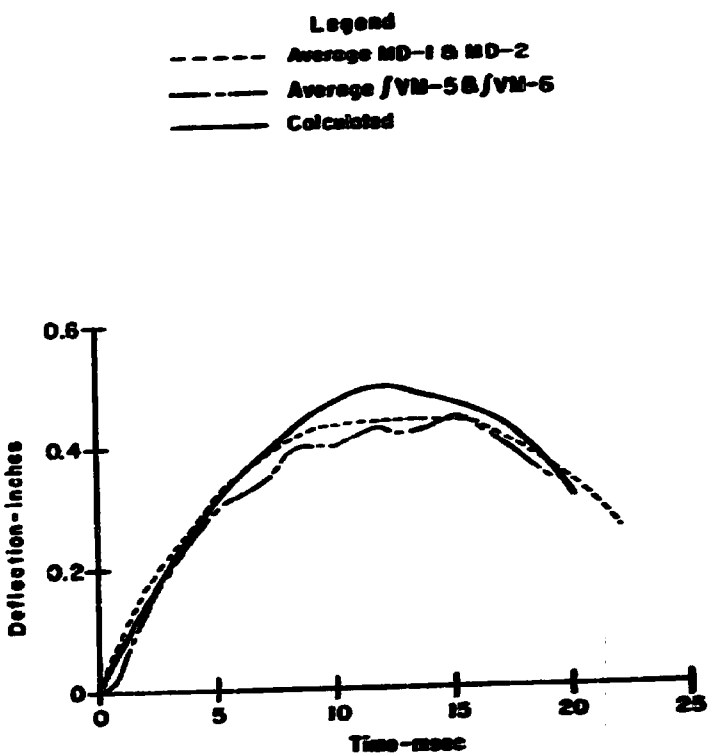

Figure 27 - Relative Deflection Histories - Test 2

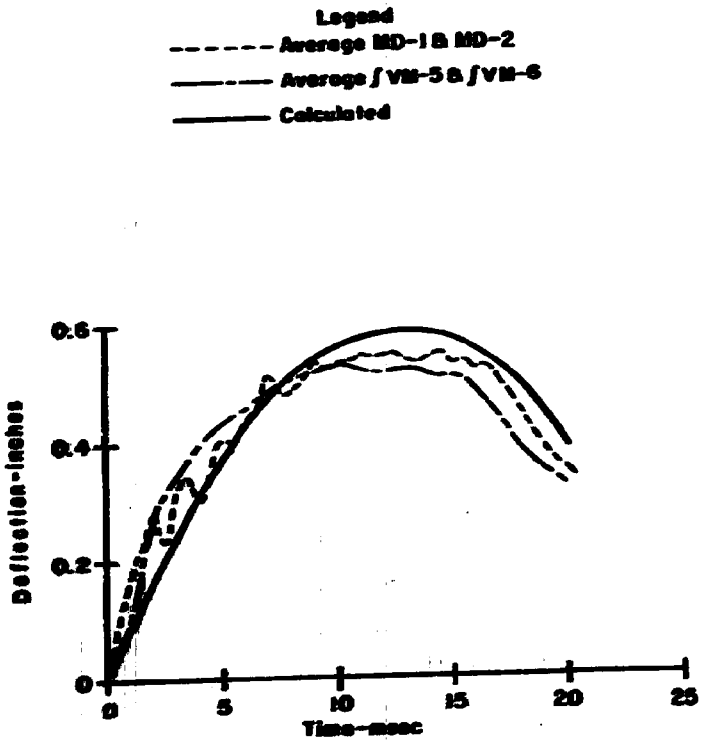

Figure 28 - Relative Deflection Histories - Test 3

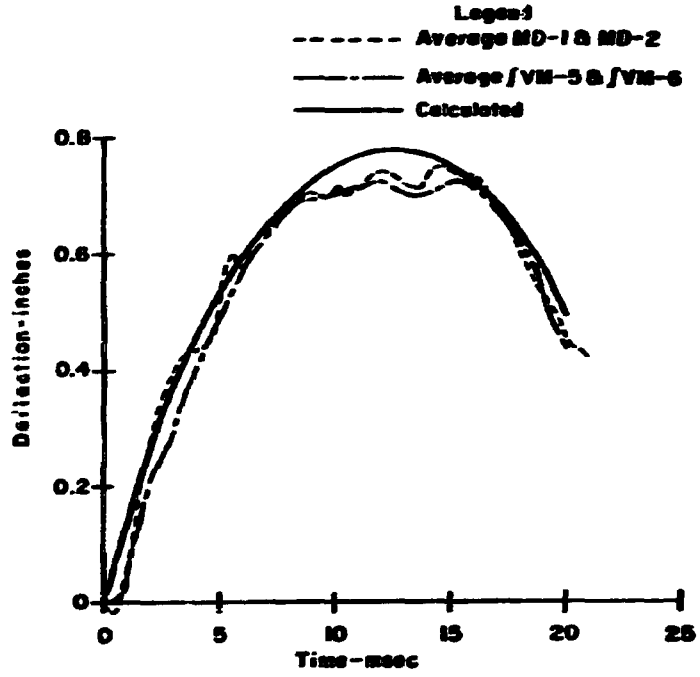

Figure 29 - Relative Deflection Histories - Test 4

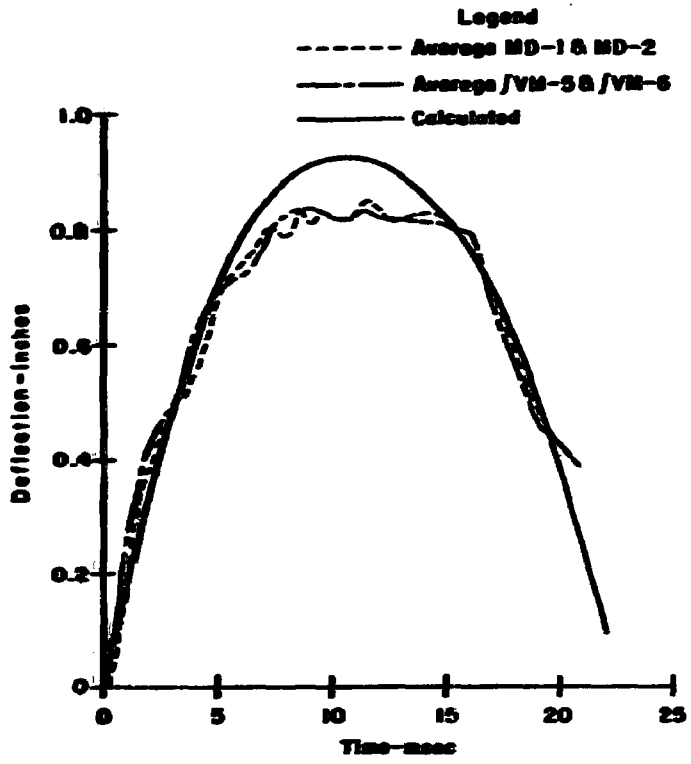

Figure 30 - Relative Deflection Histories - Test 5

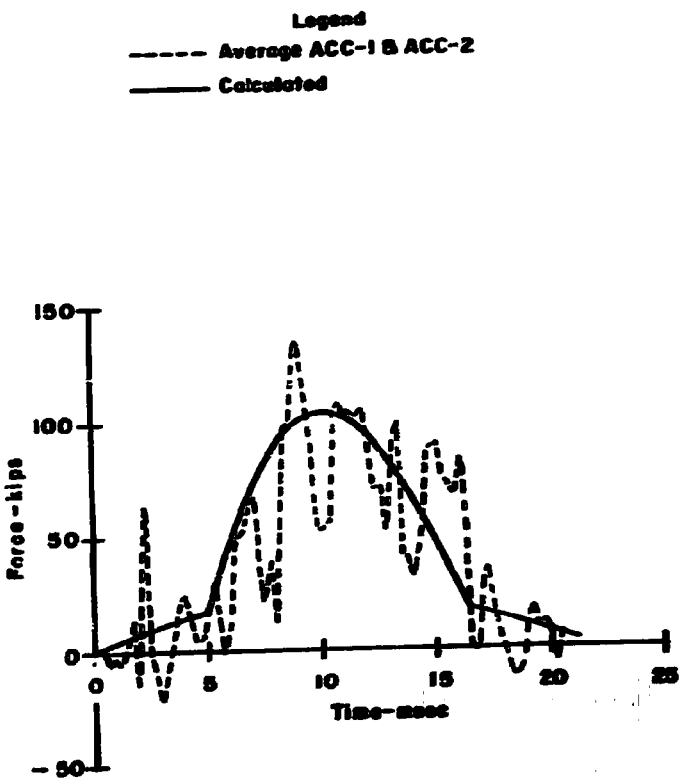

Figure 31 - Force-Time Histories - Test 2

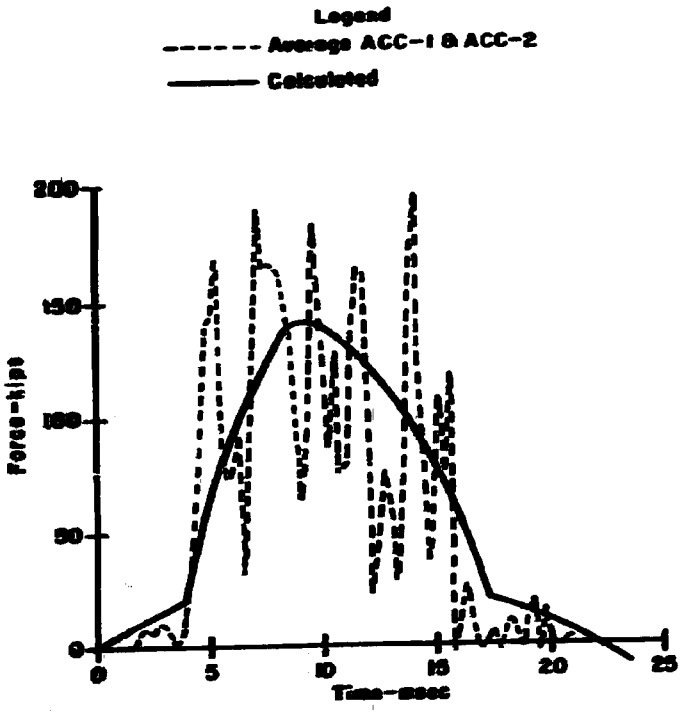

Figure 32 - Force-Time Histories - Test 3

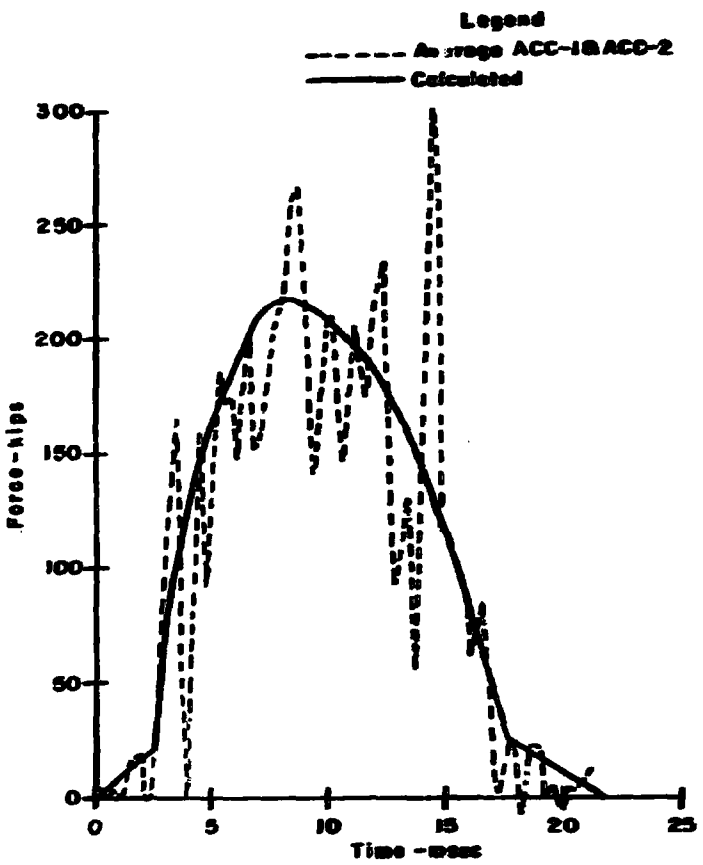

Figure 33 - Force-Time Histories - Test 4

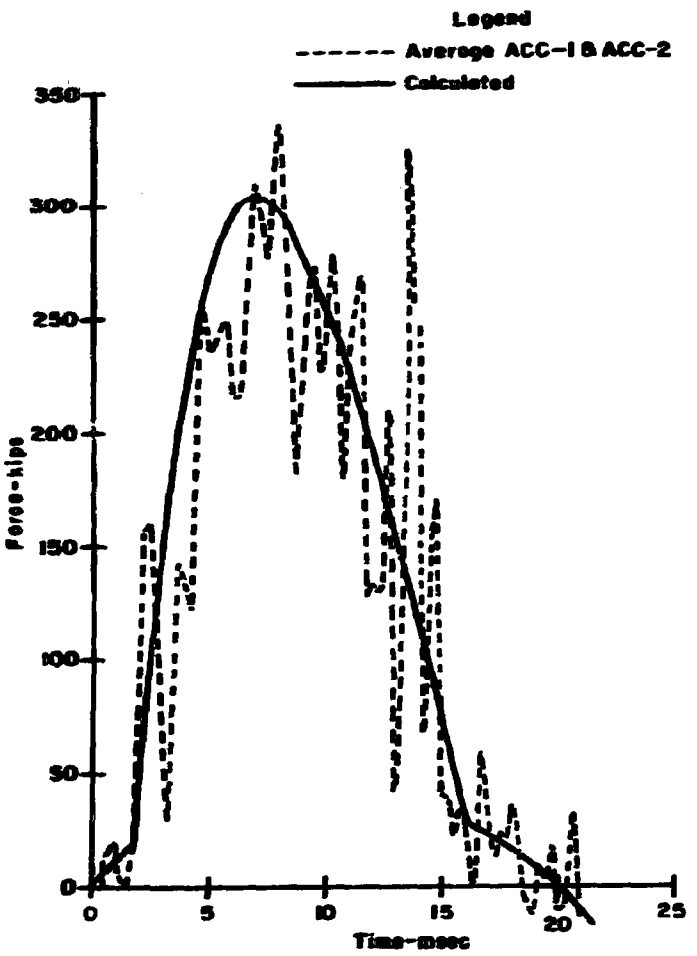

Figure 34 - Force-Time Histories - Test 5

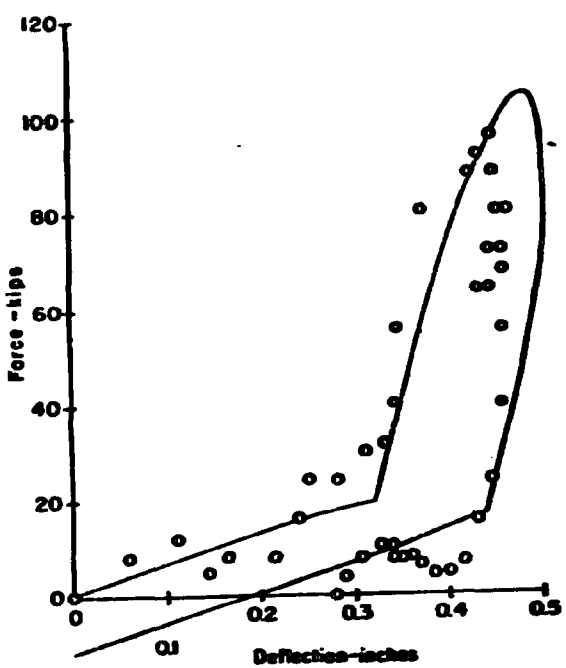

Figure 35 - Force-Deflection Curve - Test 2

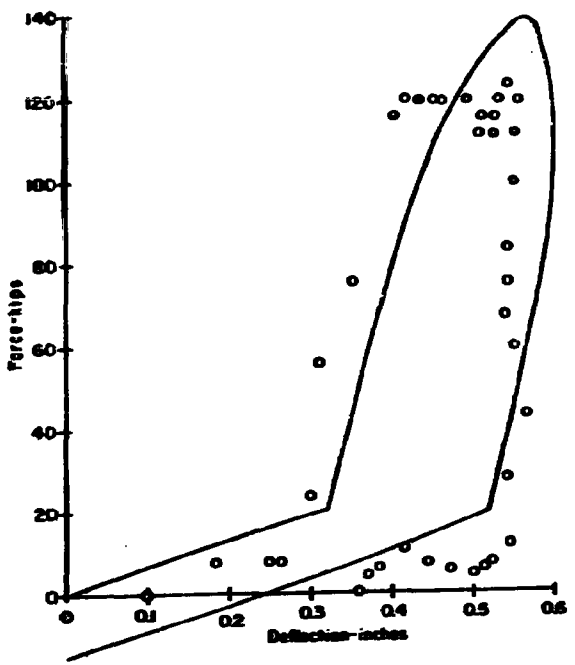

Figure 36 - Force-Deflection Curve - Test 3

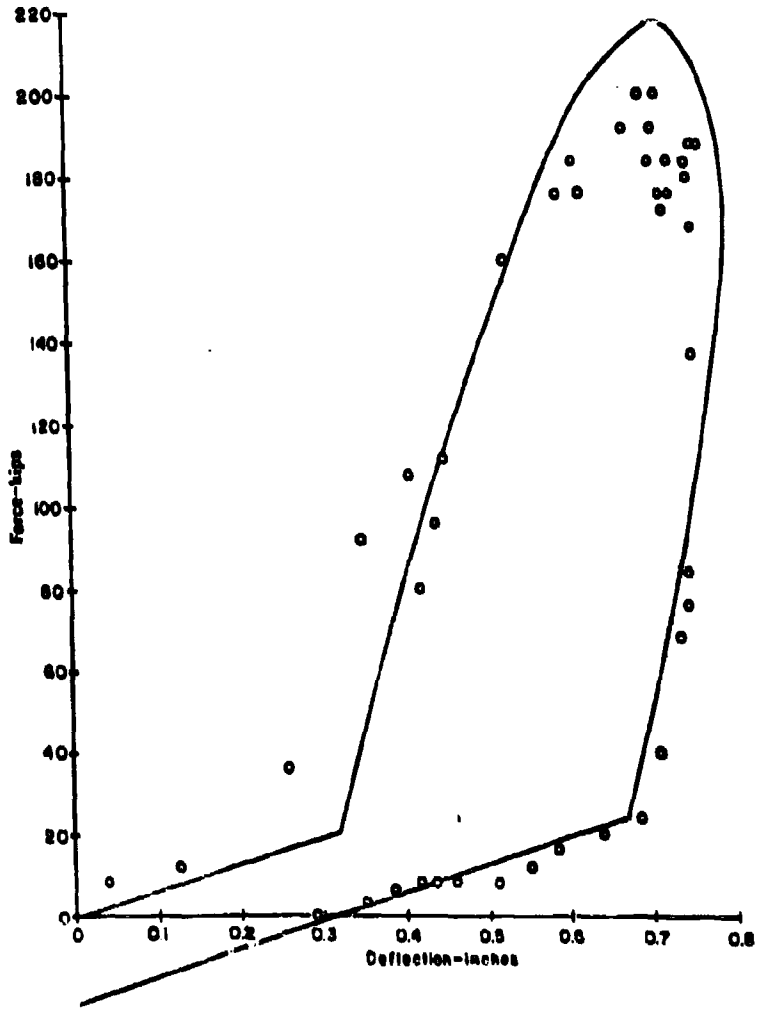

Figure 37 - Force-Deflection Curve - Test 4

The results shown in Figures 23 through 38 show an agreement between theory and experiment which is about as good as the agreement of the experimental measurements with themselves. This is indicated by the comparison of sum of mass and relative velocities with base velocities (Figures 19 through 22), integral acceleration curves with velocity curves (Figures 23 through 26), and integral velocity curves with deflection curves (Figures 27 through 30). The maximum error is less than 11 percent of the maximum value of the variable.*

* The high frequency spikes in the acceleration are not considered since they do not represent rigid body motions of the mass.

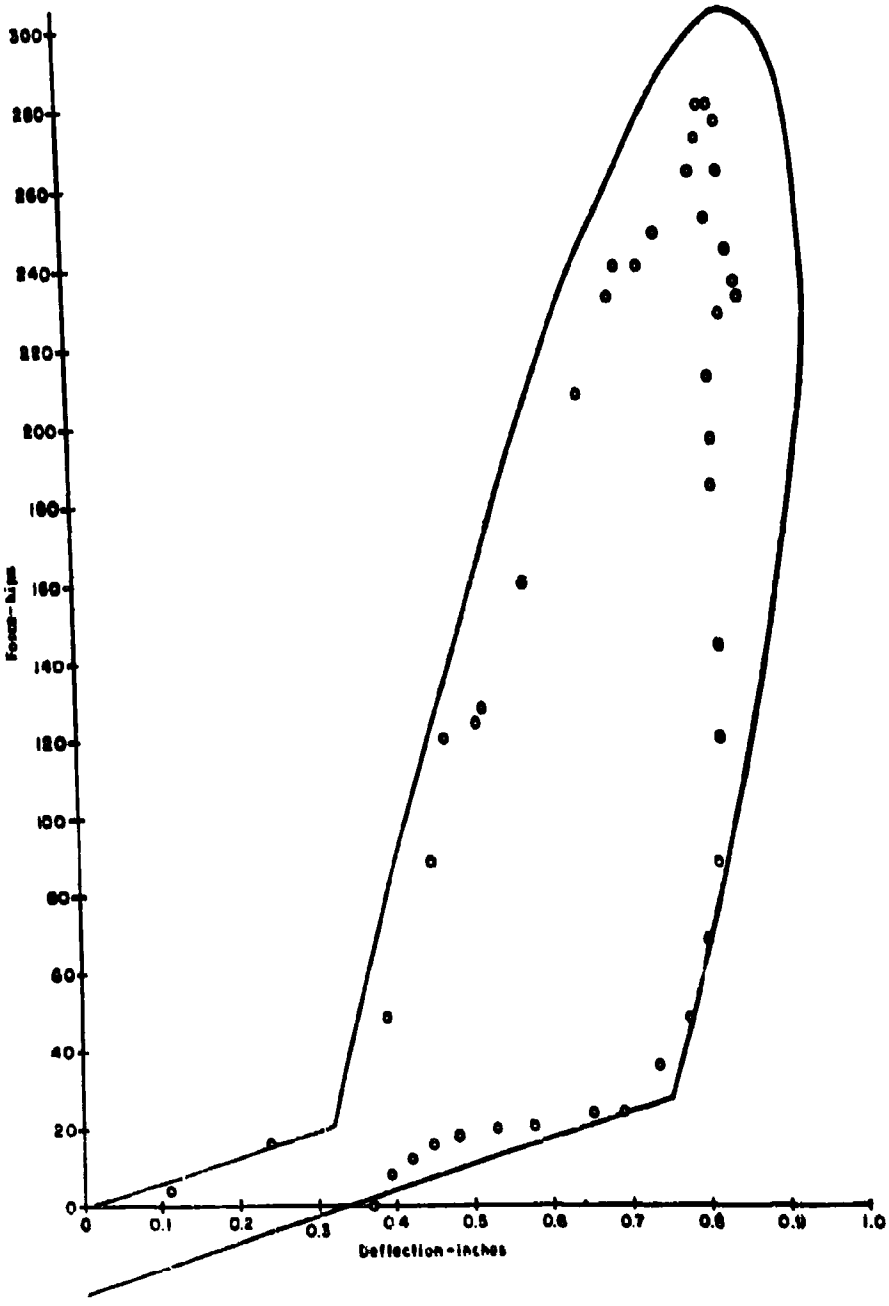

Figure 38 - Force-Deflection Curve - Test 5

DISCUSSION OF RESULTS

The shock tests of the 5M10,000-H resilient mounts using the concentrated mass have provided considerable insight into the behavior of the mount under dynamic conditions. The test results have shown that the dynamic behavior of the mounting system under shock was controlled, as expected, by the action of the snubber components. During early shock motions, before snubber engagement, the shear and compression components were compressed but transmitted only small forces in comparison to the later forces attributed to the snubber action. The forces transmitted by the shear and compression components were not clearly defined by the instrumentation histories before the initial snubber engagement because of their small magnitudes. Consequently, the force data given for the early deflections on the dynamic force-deflection curves were not as accurate as during the periods of snubber engagement. The shear and compression components behaved in a similar manner during the periods between the upper snubber disengagement and the lower snubber engagement. During this interval, also, the forces were small and were not clearly defined. The deflection at which the force returned to zero on the force-deflection curve was questionable for this reason. However, throughout the major interval of snubber compression the forces were described more accurately and consequently more confidence may be placed in these results.

Each of the dynamic force-deflection curves began to show a sharp increase in force after the snubber clearance of 0.31 inch was closed. After this deflection, the dynamic force increased rapidly with increasing deflection. The force increased until the maximum value was reached at a deflection somewhat lower than the maximum deflection. After the maximum force was reached the force decreased slightly as the deflection approached its maximum value. As the maximum deflection was attained the force dropped quite rapidly at almost constant deflection. Thereafter, the force decreased more slowly with decreasing deflection until the force dropped to zero. This force-deflection relation showed a large amount of energy absorption which indicated that significant damping was present in the mounts. Evidence indicated that the snubber did not return to its original shape during its expansion. Thus, the force reached zero at a deflection greater than 0.31 in., which was to be expected for a damped system under dynamic loading. The force data were somewhat inaccurate in this region; hence, the force-deflection curves were not consistent concerning the set deflection.

The magnitude of the maximum forces and maximum deflections experienced by the mounts varied with attack severity. The maximum force varied from about 100,000 lb to 275,000 lb; the maximum deflection increased from 0.45 to 0.84 inch. Both of these quantities increased with increasing shock factor. This increase for each quantity was almost linear when plotted against shock factor for the attack severities considered. This variation is shown in Figures 39 and 40.

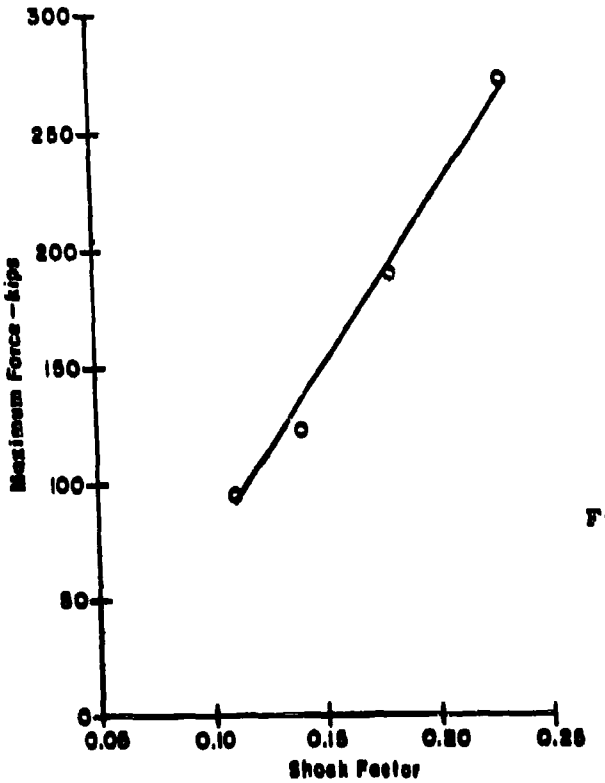

Figure 39 - Maximum Force versus Shock Factor

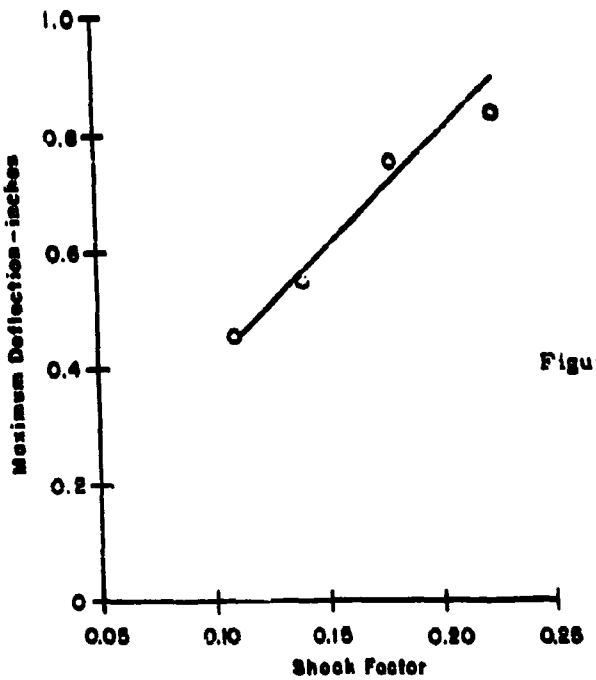

Figure 40 - Maximum Deflection versus Shock Factor

For the most part, the results of these tests and the results obtained from the FSP tests of the propulsion turbine (See Appendix A) showed general agreement. The overall action of the mounts proved to be the same in each case. There were, however, some disagreements between the force-deflection curves obtained from the two series of tests. The most apparent of these discrepancies lies in the shape of the force-deflection curves. Nevertheless, the maximum values of force and deflection between the two series of tests showed reasonable agreement. The discrepancy in the shapes of the curves may be attributed to the difficulty in measuring accelerations accurately. The tests using the lead weight gave a considerable improvement over the propulsion turbine tests; however, in regions of low acceleration an accurate measurement of the history remained a difficult task.

A comparison of the dynamic force-deflection curves and the static force-deflection curve (Figures 13-16) reveals a number of significant differences. The static force-deflection curve was characterized by the fact that the force increased with increasing deflection as the deflection approached a nearly vertical asymptote. The asymptote was approached at relatively low levels of force and essentially established the maximum deflection to be almost independent of the applied force. The shape of this force-deflection curve has led a number of writers to represent it mathematically by the tangent function. One of the major differences between the static and dynamic force deflection characteristics was that the static behavior was specified by one distinct nonlinear force-deflection curve whereas the dynamic behavior was specified by a family of curves which are a function of the loading rate (attack severity). However, as discussed previously, the maximum force and maximum deflection increased linearly with increasing attack severity.

To compare the effects of using the static and dynamic force-deflection curves the maximum force and deflection were calculated for the last four tests using the static force-deflection curve for increasing load, Figure 56. These results are compared with measurements and dynamic calculations in Table 5. Since the maximum measured point on the static curve was insufficient for the calculations except for Test 2, the curve was extrapolated by a line tangent to it at 0.85 in., 160 kips. Therefore these calculated values should be upper bounds on deflection and lower bounds on forces for calculations based on the static curve. The results in Table 5 show in each case a higher deflection and except for Test 2 a higher force than either the experimental results or calculated results using the model of Figure 18. The maximum error in the calculated deflection using the static force-deflection curve was about 75 percent for Test 2 and decreased with increasing attack severity to 21 percent for Test 5. The error in the calculated maximum force, however, which was small for Test 2, increased with increasing attack severity to more than 100 percent for Test 5.

TABLE 5
Maximum Forces and Relative Deflections

Comparisons		Method of Determination		
		Experimental	Dynamic Curve	Static Curve
Test 2	Force (kip)	97	103	85
	Deflection (in.)	0.46	0.50	0.80
Test 3	Force (kip)	124	138	220
	Deflection (in.)	0.55	0.60	0.88
Test 4	Force (kip)	192	217	410
	Deflection (in.)	0.76	0.78	0.95
Test 5	Force (kip)	273	305	660
	Deflection (in.)	0.84	0.95	1.02

A comparison of the 5M10,000-H mount assembly responses under shock load with that of a pair of three-element linear systems, Figure 18, under a base motion representing that of the actual mount, confirms that there is no direct relation between the dynamic force-deflection curves and the static force-deflection curve. Each element of the mount under vertical deflection can be satisfactorily represented by a three-element system shown in Figure 17.

The existence of the dynamic force-deflection characteristics for the resilient mounts eliminates the possibility of using the static characteristics alone to predict the dynamic response of supported equipment. Some analytical studies[6] of the nonlinear shock problem have been made using the tangent representation of the mount stiffness. These results should be reconsidered in light of the great differences between the static and dynamic characteristics of the mounts.

GENERAL CONCLUSIONS

This investigation of the performance of a type 5M10,000-H resilient mount assembly under vertical shock loading has provided insight into their behavior under dynamic conditions. From the documented behavior of the resilient mounts during this series of tests and the analysis based on the system of Figure 18, the following conclusions have been drawn:

1. The force-deflection relationships of the resilient mount under dynamic conditions cannot be obtained from static tests alone.

2. The maximum forces and maximum deflections under shock increase almost linearly with increasing attack severity for the range of attacks considered.

3. Dynamic force-deflection curves must be used in calculations of the response of supported equipment under vertical shock loading.

4. The action of the 5M10,000-H mount under vertical shock loading can be adequately represented by parallel systems consisting of two springs and a dashpot. Linear elements were sufficient for the range of attacks considered.

REFERENCES

1. "Shock and Vibration Handbook," Edited by C. M. Harris and C. E. Crede, Vol. 2, McGraw-Hill, Toronto, London and New York (1961). "Rubber Springs," (William A. Frye), pp. 35-2, 35-8.

2. Oliver, R. E., "Shock Testing of General Electric SS(N)-Type Submarine Propulsion Turbine on the Floating Shock Platform," David Taylor Model Basin Report 1800, November 1963.

3. Morris, R. E., "Development of 10,000-Pound Capacity Mounting-Evaluation of 5M10,000 Mounting System," Rubber Laboratory, Mare Island Naval Shipyard Report 9-94 (25 July 1958).

4. Treloar, L. R. G., "The Physics of Rubber Elasticity," Second Edition, Oxford University Press, Amen House, London (1958), p. 342.

5. Goldsmith, Werner, "Impact The Theory and Physical Behaviour of Colliding Solids," Edward Arnold Ltd., London (1960), p. 24.

6. Snowdon, J. C., "Response of Nonlinear Shock Mountings to Transient Foundation Displacements," The Journal of the Acoustical Society of America, Vol. 33, No. 10, pp. 1295-1304 (October 1961).

7. "Shock Tests, H. I. (High Impact), Shipboard Machinery, Equipment and Systems, Requirements for," MIL-S-901C(NAVY), 15 January 1963.

8. "Mount, Resilient, Type 5M10,000-H," MIL-M-21649A(SHIPS), 13 September 1960.

APPENDIX A

Preliminary Evaluation of SM10,000-H Resilient Mounts

INTRODUCTION

Under the requirements of the current shock test specification[7] the David Taylor Model Basin tested a General Electric SS(N) Type Submarine Propulsion Turbine on the Floating Shock Platform. For these tests,[1] the turbine was resiliently mounted by four Type 5M10,000-H mounts. This installation presented an opportunity to obtain some preliminary information on the behavior of the mounts in an installation simulating shipboard conditions.

TEST PROCEDURE

The turbine was installed on a subbase simulating the prototype structure in way of the turbine. The subbase, in turn, was supported by four Type 5M10,000-H resilient mounts attached to a stiff foundation structure welded to the inner bottom of the Floating Shock Platform. A view of the foundation and subbase installation on the Floating Shock Platform is shown in Figure 41 and the completed installation is shown in Figure 42.

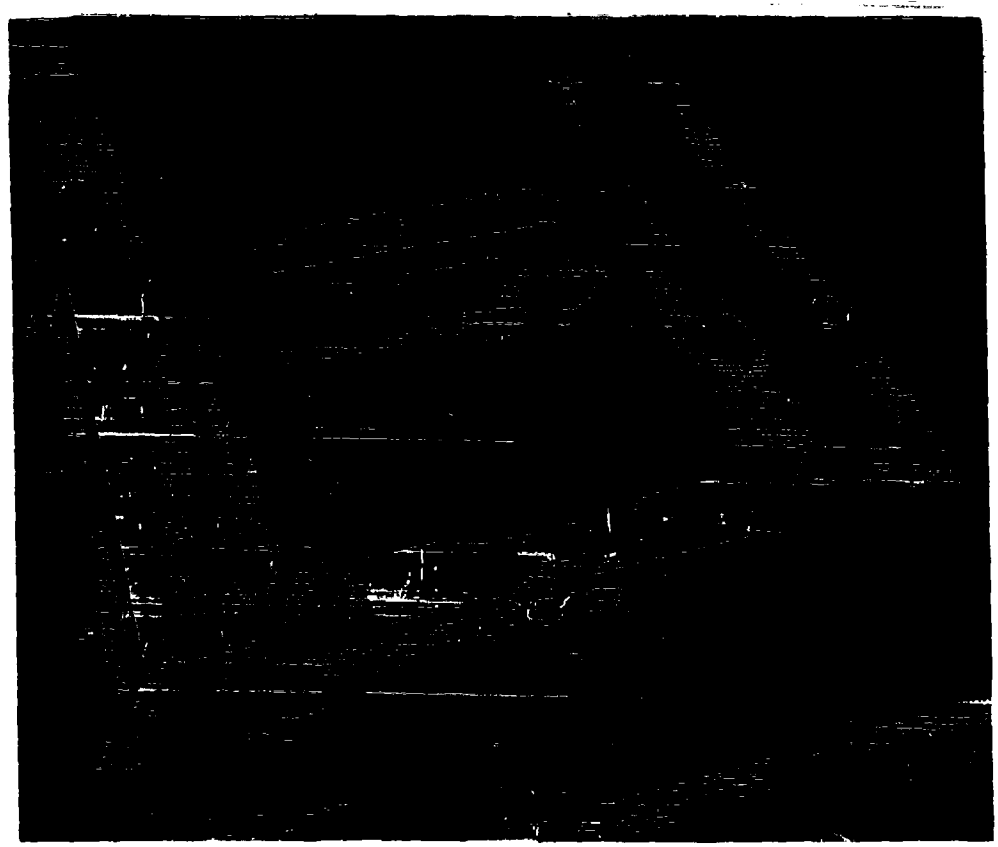

Figure 41 - Installation of Foundation Subbase

Figure 42 - Equipment Installation on Floating Shock Platform

The completed installation was instrumented with a number of velocity meters (VM) and mechanical deflection gauges (MD). The locations were selected to measure the input to the foundation, response of the subbase-turbine structure, and the excursions of the mounts. The locations of the gauges are shown schematically in Figure 43 and are listed in Table 6.

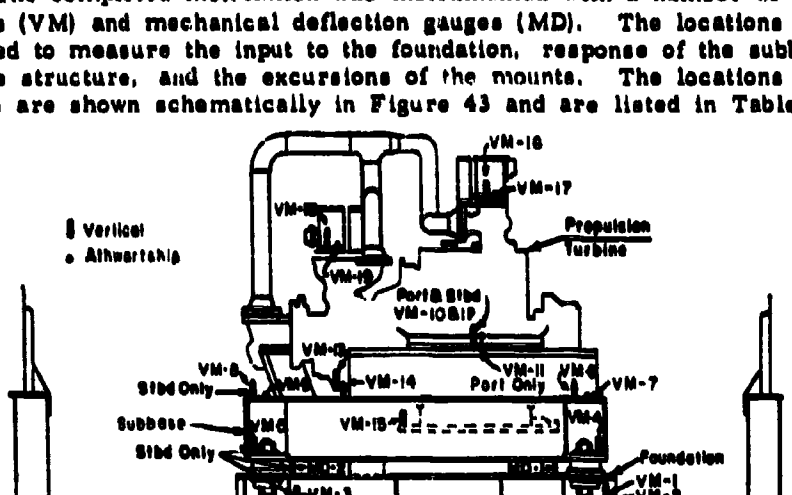

Figure 43 - Instrumentation Locations

TABLE 6
Gauge Locations

Gauge	Position	Location
VM-1	Vertical	FRP deck at intersection of Fr 3 and L-2 (port)
VM-2	Athwartship	FRP deck adjacent to VM-1
VM-3	Vertical	FRP deck at intersection of Fr 6 and L-2 (starboard)
VM-4	Vertical	Subbase adjacent mount bolt (port side forward)
VM-5	Vertical	Subbase adjacent mount bolt (starboard side aft)
VM-6	Vertical	Top of subbase port side forward
VM-7	Athwartship	Adjacent to VM-6
VM-8	Vertical	Top of subbase starboard side aft
VM-9	Athwartship	Adjacent to VM-8
VM-10	Vertical	Port side support flange
VM-11	Athwartship	Adjacent to VM-10
VM-12	Vertical	Starboard side support flange
VM-13	Vertical	Top of flex plate
VM-14	Athwartship	Adjacent to VM-13
VM-15	Vertical	Exhaust flange
VM-16	Vertical	Astern steam chest cover
VM-17	Athwartship	Adjacent VM-16
VM-18	Vertical	Ahead steam chest cover
VM-19	Athwartship	Adjacent to VM-18
MB-1	Vertical	Adjacent to shock mount port side forward
MB-2	Vertical	Adjacent to shock mount starboard side aft

Photographs of typical installations are shown in Figures 44 and 45. (It should be noted that the designation and location of these instruments are different from those described in the main body of this report.)

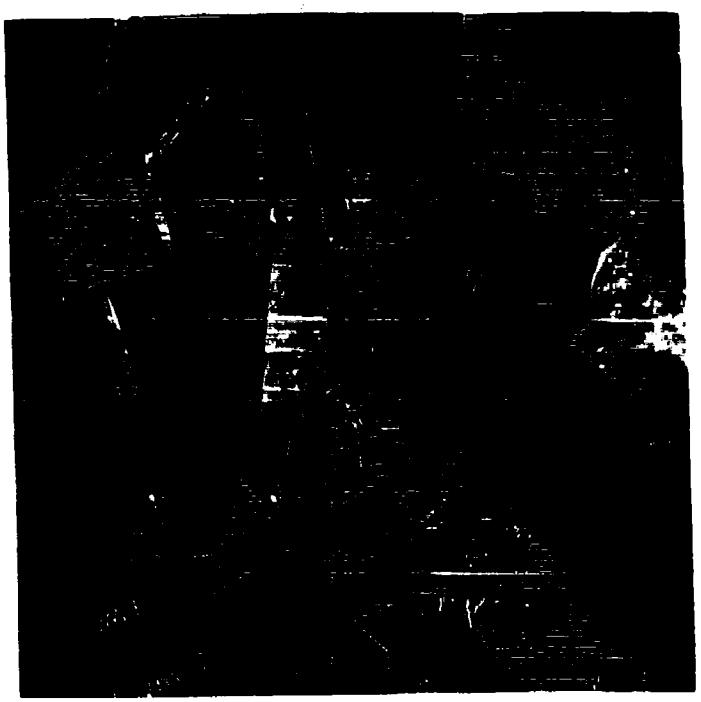

Figure 44 - Typical Instrumentation on Floating Shock Platform Inner Bottom and Subbase

Figure 45 - Typical Velocity Meter Installations on Turbine Bolting Flange

Five underwater explosion shock tests of increasing severity were conducted against the Floating Shock Platform. A schematic of the test geometry is presented in Figure 46 and the test geometries and input velocities are tabulated in Table 7.

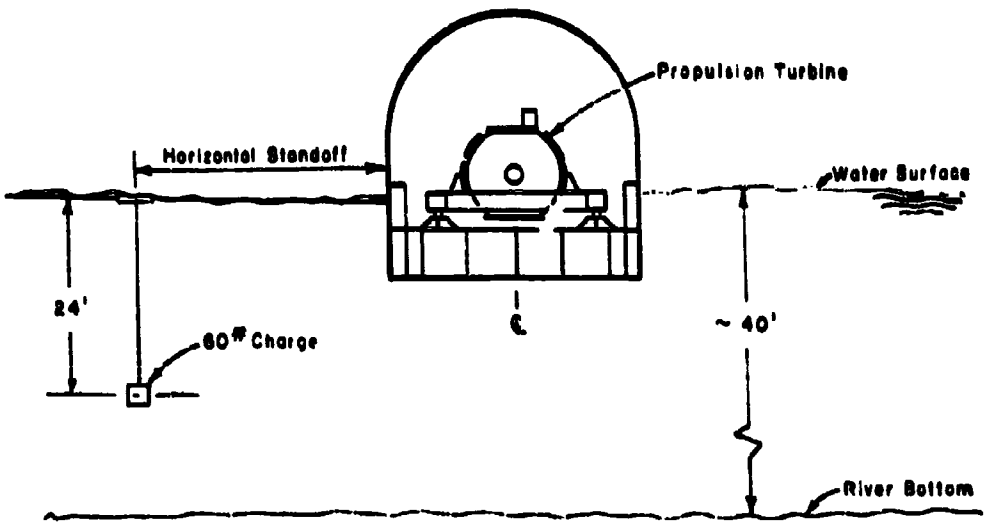

Figure 46 - Test Geometry

TABLE 7
Test Geometries

Test No.	Horizontal Standoff	Charge Depth	Charge Weight	Peak Input Velocity*
	ft	ft	lb	fps
1	60	24	60	5
2	40	24	60	8
3	30	24	60	11
4	25	24	60	13
5	20	24	60	15

*Recorded at base of foundation on the attack side (VM-1).

RESILIENT MOUNT BEHAVIOR

The experimental results were studied to seek an understanding of the sequence of events under shock and the determination of the relations between the forces transmitted by the mounts and the deflections experienced.

The examinations of the various velocity histories indicated that the motion of the subbase-turbine structure consisted of a vertical translation during the early phase of the shock motion. During later phases of the response rigid body rotations occurred as well; however, these motions were of a low frequency and were not appreciable during the early behavior of the mounts.

Velocity histories were studied and correlated with the deflection histories to obtain an understanding of the sequence of events occurring during the shock response. These correlations indicated that essentially no motion was experienced by the subbase-turbine structure until the upper snubber engaged. Subsequently, the structure underwent a vertical acceleration during the period in which the snubber was compressed. Upon the disengagement of the upper snubber the structure tended to move with constant velocity until the lower snubber engaged and introduced a deceleration and a consequent decrease in velocity occurred.

As explained above, the initial phase of the shock response was characterized by a sudden vertical acceleration of the subbase-turbine structure. Figure 47 presents four typical velocity histories from Test 5 to illustrate the shock input and shock response. These plots represent, first, the input to the foundation (VM-1); next the response at subbase (VM-4); then, the response of the turbine at the attachment flange (VM-10); and finally, the response near the top of the turbine at the astern valve (VM-16). A comparison of the velocity histories at the various points on the subbase-turbine structure given by VM-4, VM-10, and VM-16 indicates that the assembly is responding as an elastic structure, i.e., the velocity and acceleration histories vary throughout the structure. Because of this velocity distribution, a rigid-body velocity history for the structure can only be approximated for purposes of determining the forces transmitted by the mounts. Meters VM-10 and VM-12, mounted on the relatively rigid attachment flange of the turbine, were selected for this approximation.

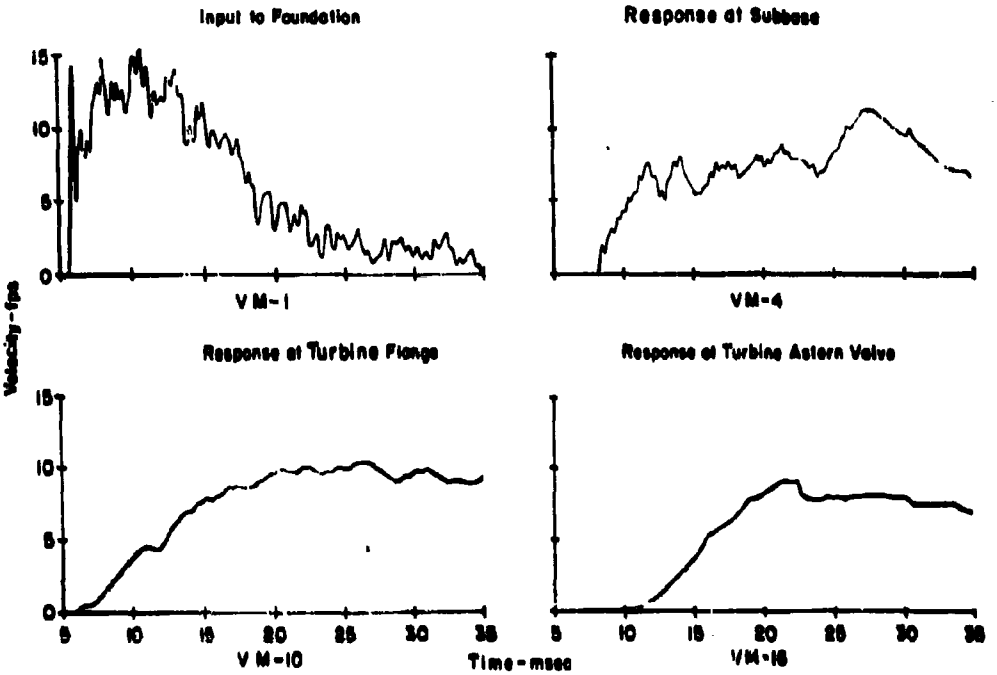

Figure 47 - Typical Velocity Histories

To determine the forces transmitted by the mounts, vertical accelerations of the subbase-turbine structure were found by measuring the slopes of the velocity history obtained by using an average of VM-10 and VM-12. An average of the two records was used to eliminate the effects of any possible port-to-starboard rotation. In a similar manner two port and starboard deflection gauges, MD-1 and MD-2, were averaged to give a corresponding vertical deflection history. With time as the common parameter, values of average acceleration and average displacement were read from these histories for the time interval of the first engagement of the upper snubber. The accelerations were then converted to forces by assuming that each mount accelerated one-fourth of the total weight of 32,000 lb. Force-deflection curves were constructed following this procedure for each test with the exception of Test 1. On this test there was some question as to whether the starboard snubbers actually engaged. Because of this complication Test 1 was disregarded and force-deflection curves were found for only Tests 2 through 5. The force-deflection curves are given in Figures 48 through 51 together with the static curve from Appendix B.

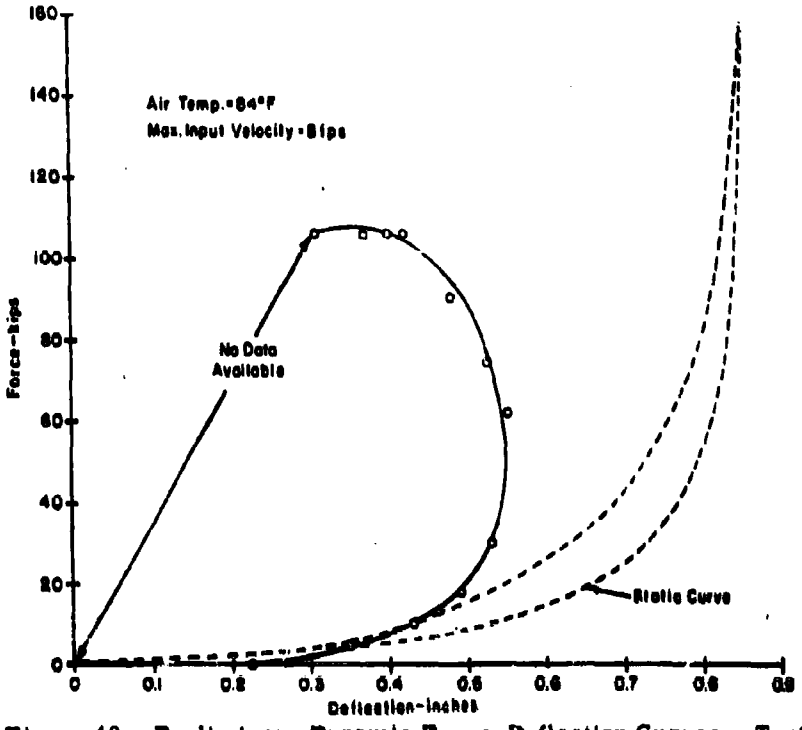

Figure 48 - Preliminary Dynamic Force-Deflection Curves - Test 2

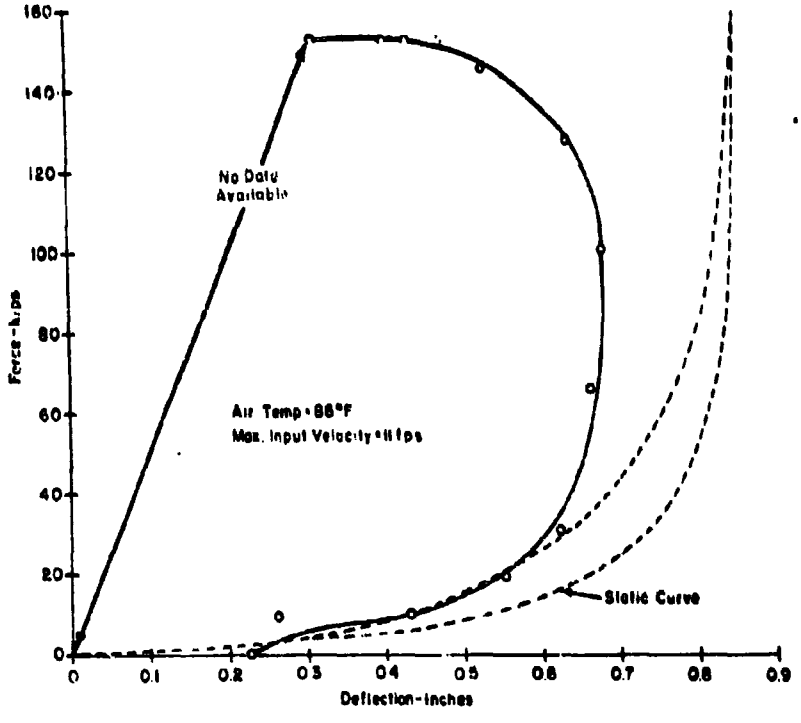

Figure 49 - Preliminary Dynamic Force-Deflection Curves - Test 3

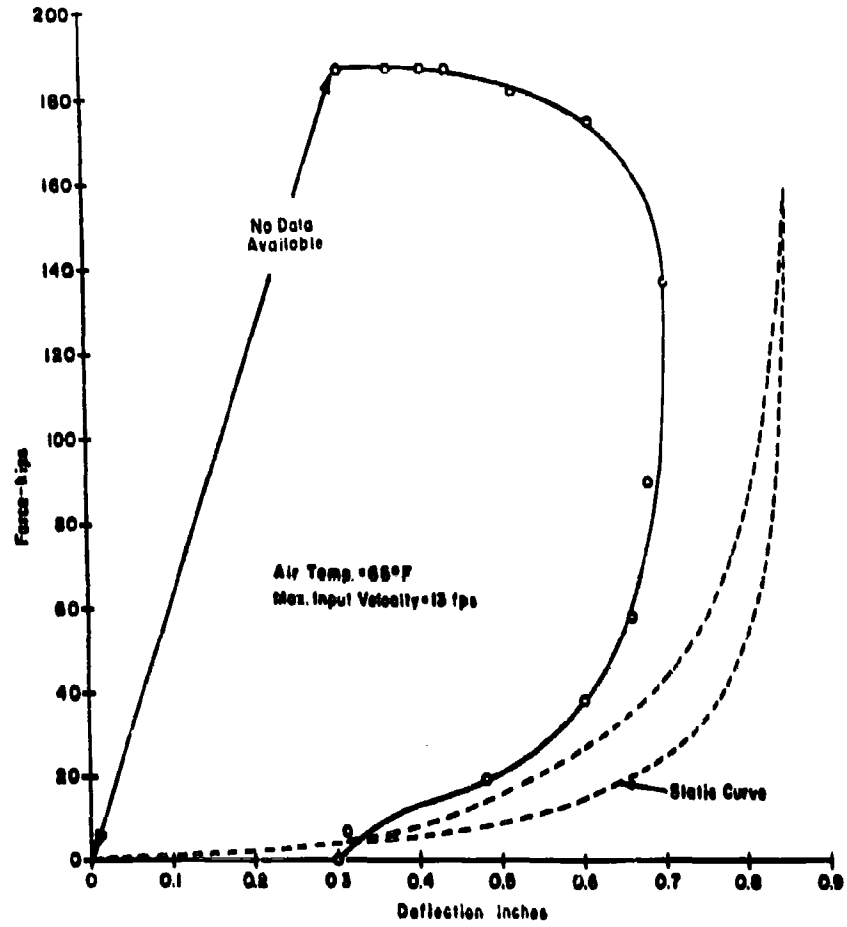

Figure 50 - Preliminary Dynamic Force-Deflection Curves - Test 4

DISCUSSION OF RESULTS

The preliminary dynamic force-deflection curves indicate that the dynamic forces are considerably larger than the corresponding static result. These results show that the largest force occurs upon snubber engagement with very small snubber deflection. After the large initial force, the force decreases as snubber deflection increases. This decrease occurs slowly at first and then more rapidly as the maximum displacement is reached. After the maximum displacement, the force decreases with decreasing deflection until the force returns to zero at a set deflection.

The force-deflection curve depends, of course, on the determination of the instantaneous acceleration of the equipment as the mount deforms.

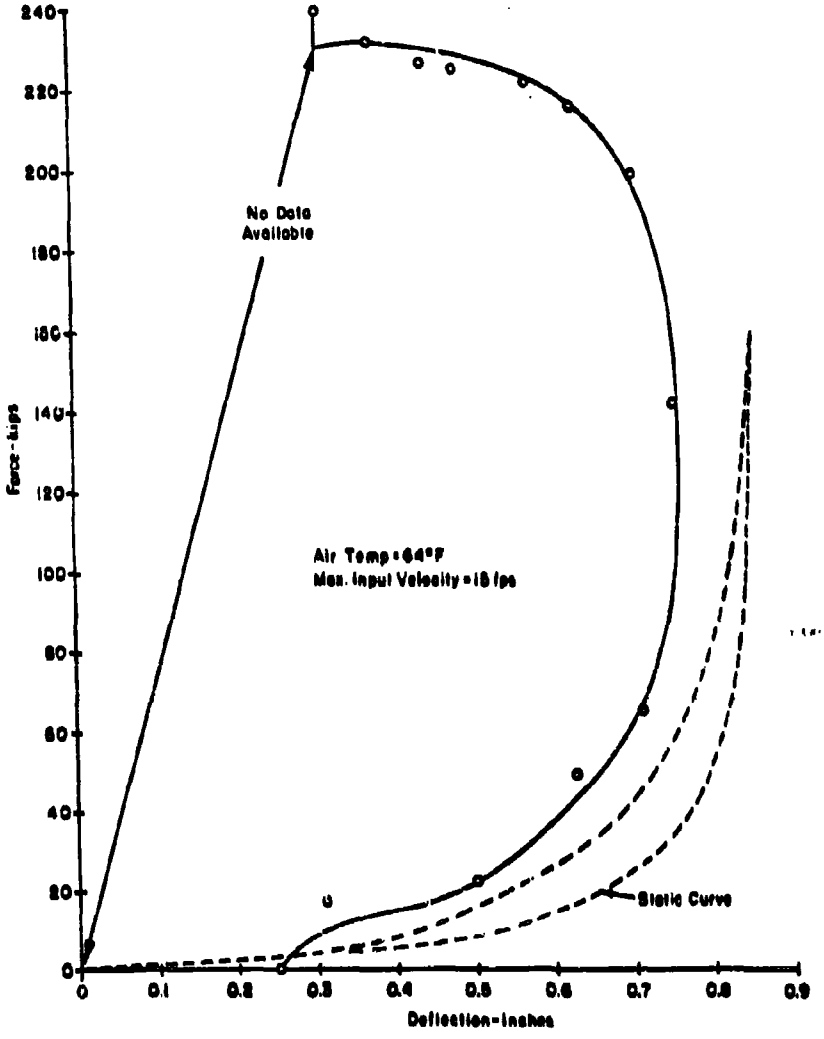

Figure 51 - Preliminary Dynamic Force-Deflection Curves - Test 9

In the present tests, it was not possible to determine the accelerations accurately from the velocity histories (See Figure 47) during the period of time in which the snubber clearance is closed and when the snubber first engages. During this time, the velocity histories show an almost discontinuous acceleration history as the snubber engages. Because of this, force data are not available until after the snubber engages and each force-deflection curve shows a discontinuity at the deflection of 0.31 inch.

The force-deflection curves obtained from these tests are intended to be preliminary results. The procedures followed in reducing these data required a number of assumptions, and the data from which these results were obtained were not entirely adequate for the purposes of this evaluation. However, the results do give some preliminary information on performance of the mounts in simulated shipboard conditions.

APPENDIX B

Static Tests of 5M10,000-H Resilient Mount

INTRODUCTION

Static tests of components of the 5M10,000-H were conducted in accordance with military specification tests.[8] The tests consisted of compressing the mount components in a vertical direction with the components installed in a test fixture simulating the shipboard loading conditions.

TEST PROCEDURE

The shear and compression components of each resilient mount were tested simultaneously in a test fixture designed to subject each component to the same deflection. By loading the components in this way a combined force-deflection for the two components was obtained. The two components installed in the test fixture are shown in Figure 52. The static tests of the shear and compression components of each mount were conducted at a rate of 0.05 in/min up to a maximum 30,000-lb load. Deflections were measured by a dial indicator at 5,000-lb increments of force. Four complete loading and unloading cycles were conducted before the shock tests.

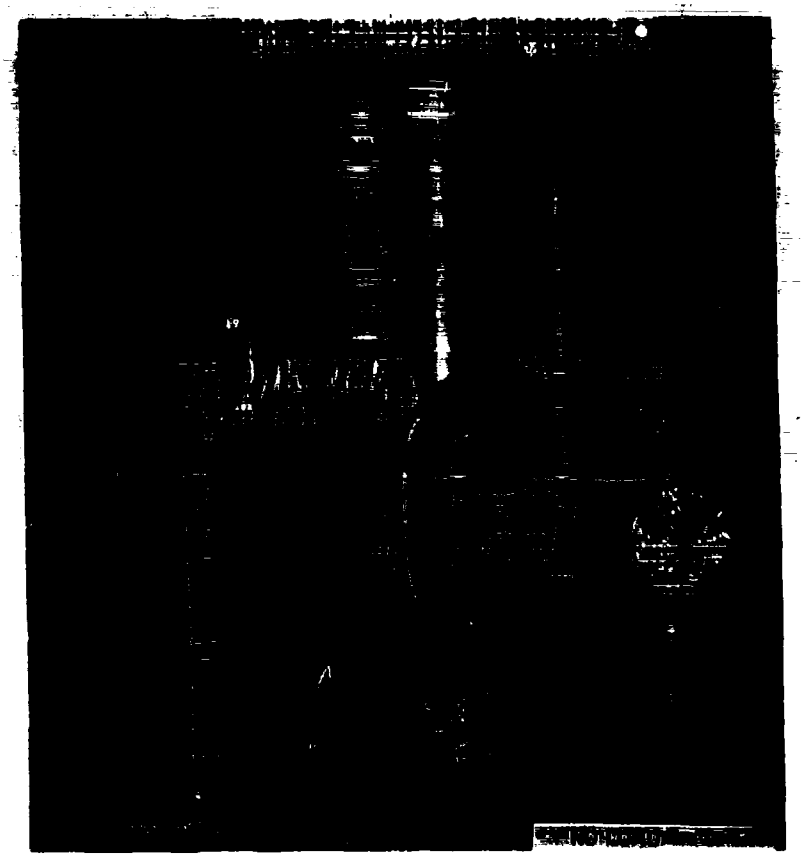

Figure 52 - Static Tests of Shear and Compression Components

Each of the snubber components was subjected to a compression test assembled in a manner simulating loading in the shock tests. The load was applied at a rate of 0.05 in/min up to a maximum 150,000-lb load. A photograph of one of the snubbers loaded to 150,000 lb is shown in Figure 53. Deflections were measured by a dial indicator at 10,000-lb increments of force. Four complete loading and unloading cycles were conducted before and after the shock tests.

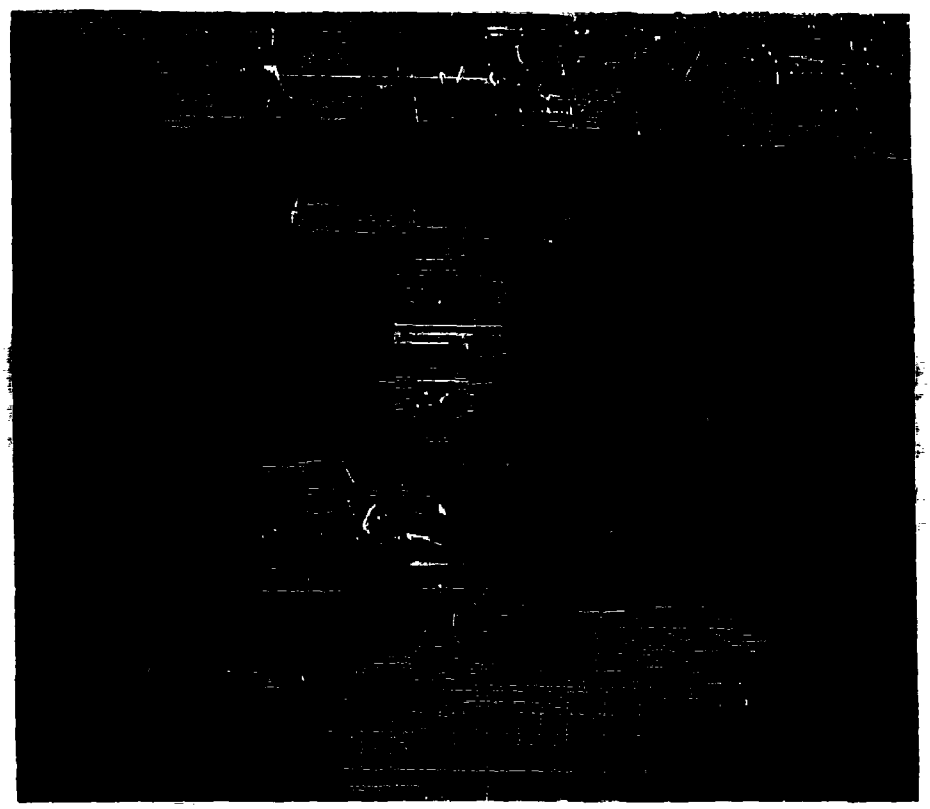

Figure 53 - Snubber Component Loaded to 150,000 Pounds

TEST RESULTS

The force-deflection curves obtained from the static tests of the shear and compression components of the two resilient mounts showed good agreement. The resulting curves could be used interchangeably with negligible error. Curves for one mount are presented in Figure 54.

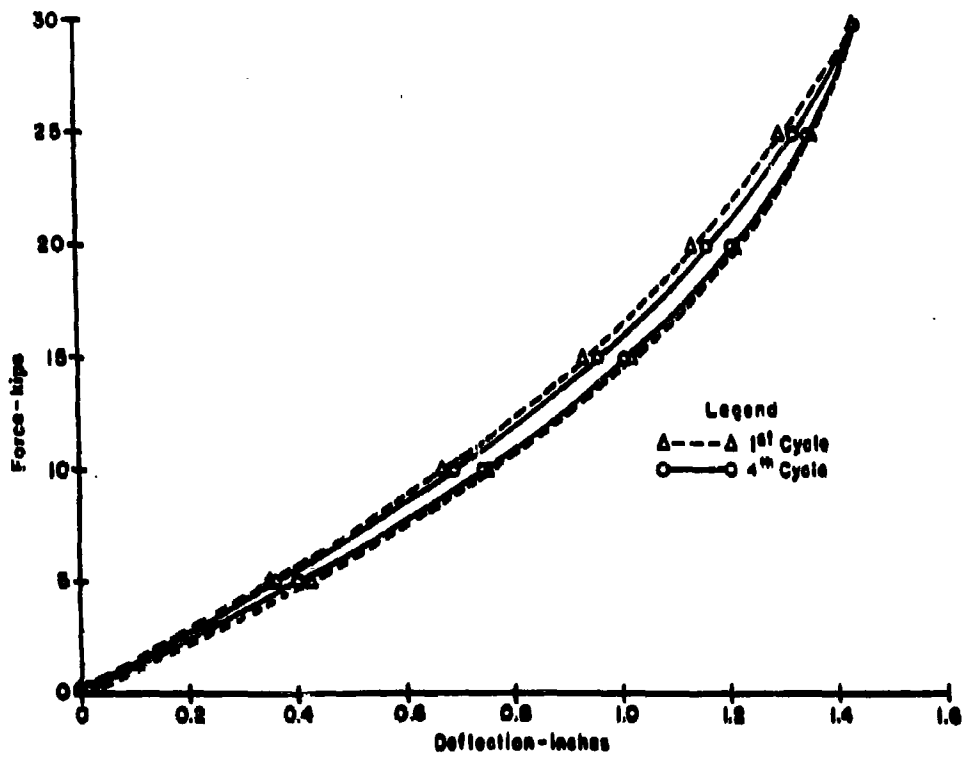

Figure 54 - Force Deflection Curves for Combined Shear and Compression Components

A force-deflection curve was obtained for each of the four snubber components before and after the shock test. For the most part the curves obtained before the shock test showed good agreement. There was some variation in the maximum deflection from snubber to snubber; this variation from the largest to the smallest deflection amounted to about 6 percent of the smallest deflection. After the shock tests, the snubbers showed better agreement; the variation was reduced to about 3 percent. The shock test did not appear to have any permanent adverse effect on the snubbers. The force-deflection curves before and after the shock tests showed good agreement. The greatest variation in maximum deflection before and after shock loading was about 3 percent. Typical force-deflection curves for one of the snubbers are shown in Figure 55.

A combined force-deflection curve for the 5M10,000-H resilient mount was found by adding the results of Figures 54 and 55. This result is given in Figure 56.

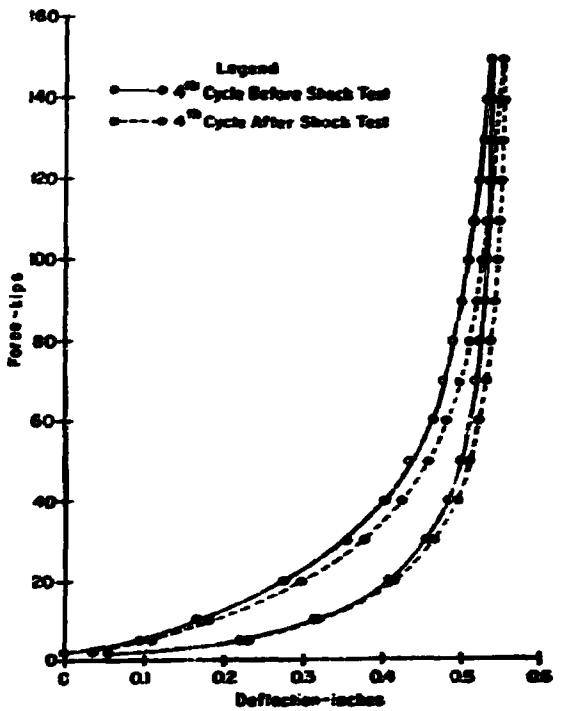

Figure 55 - Typical Force-Deflection Curves for Snubber Component

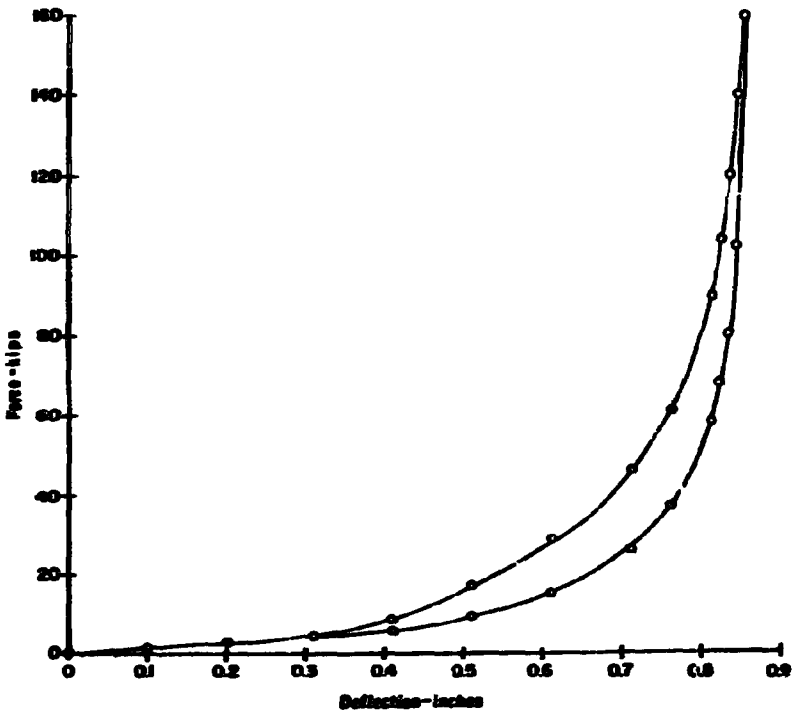

Figure 56 - Static Force-Deflection Curve for 5M10,000-H Resilient Mount Assembly

APPENDIX C

The Representation of the Compression and Shear Mounts and the Snubber on an Analog Computer

INTRODUCTION

The characteristics of the compression and shear mounts and the snubber for the shock loadings under consideration in this report can each be adequately represented by a viscous element, such as a dashpot, and two mechanical springs. To determine the numerical values which best fit each of these parameters for this specific mount and snubber, and to evaluate the adequacy of this representation, a system that would simulate one mount and one snubber as loaded in the experimental explosion test was set up on an analog computer. Also, to represent the input motion applied to this system, a set of differential equations was programmed which had as its solution an equation in time very nearly duplicating the input velocity to the mechanical system as measured in each of the explosion tests.

The purpose of this appendix is to describe the equations solved by the computer and to present the computer program used to obtain these solutions.

DERIVATION OF EQUATIONS

MATHEMATICAL MODEL FOR THE MOUNT ASSEMBLY

The mechanical system simulated for the equations is shown schematically in Figure 57; notations are listed in Table 8.

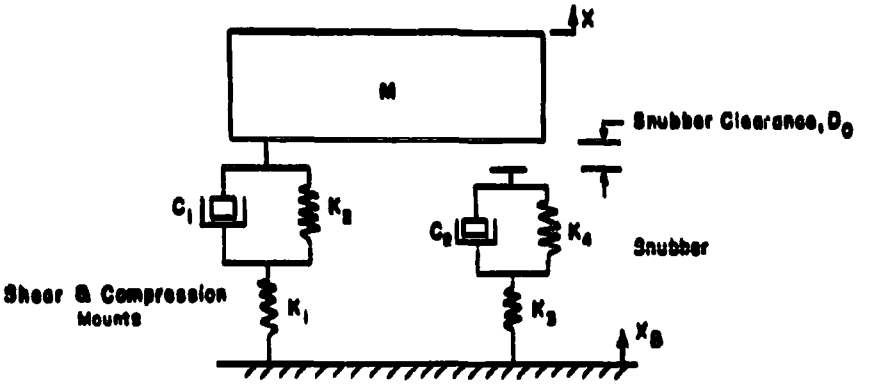

Figure 57 - Mathematical Model for the Mount Assembly

TABLE 8
Notations Used in Computer Program

Notation		Unit
A	The average deceleration of the base	ft/sec^2
B	The maximum value of the sinusoidal component of the base velocity	fps
C_1	Viscous element or dashpot associated with the mounts	kip-sec/in.
C_2	Viscous element or dashpot associated with the snubber	kip-sec/in.
D_0	Initial relative displacement between the base and the snubber which must be closed before the snubber can begin to act	in.
d	Asymptote at which the nonlinear snubber spring becomes infinitely stiff	in.
F	Total force acting on the mass; $F = F_1 + F_2$	kip
F_1	Force the mounts exert on the mass	kip
F_2	Force the snubber exerts on the mass	kip
F_4	Force exerted by spring K_4 whether linear or nonlinear	kip
K_1	Linear spring constant associated with the mounts	kip/in.
K_2	Linear spring constant having ends in common with viscous element, C_1 associated with the mounts	kip/in.
K_3	Linear spring constant associated with the snubber	kip/in.
K_4	Spring associated with snubber having characteristic selectable as linear or nonlinear; spring constant when linear characteristic selected. Has ends in common with viscous element, C_2	kip/in.
k_4	Initial slope of the characteristic of the nonlinear spring	kip/in.
M	Total mass reacting on the mount and snubber	slug
t	Time	sec
V_0	The initial velocity of the base at $t = 0$	fps
X	Absolute displacement of the mass with respect to a fixed point in space	in.
X_B	Absolute displacement of the base with respect to a fixed point in space; the input motion	in.
Z	Relative displacement between the mass and the base, $Z = X - X_B$	in.
Z_1	Relative displacement between the ends of spring K_1	in.
Z_2	Relative displacement between the ends of spring K_4 or dashpot C_1; $Z_2 = Z - Z_1$	in.
Z_3	Relative displacement between the ends of spring K_3	in.
Z_4	Relative displacement between the ends of spring K_4 or dashpot C_2	in.
β	Time scale factor at which the computer operates	dimensionless
ω	The angular frequency of the sinusoidal component of the base velocity	rad/sec

All components were considered to be linear over their range of motions with the exception of spring K_4. The computer was connected so that by throwing a switch, this spring could be made either linear or nonlinear.

With the switch in the linear position $F_4 = -K_4 Z_4$

and in the nonlinear position $F_4 = -k_4 Z_4 \left(\frac{1}{1 + \frac{Z_4}{d}}\right)$.

The shape of this nonlinear curve and the fit as compared to an experimentally determined static force-deflection curve obtained for a snubber may be seen in Figure 58.

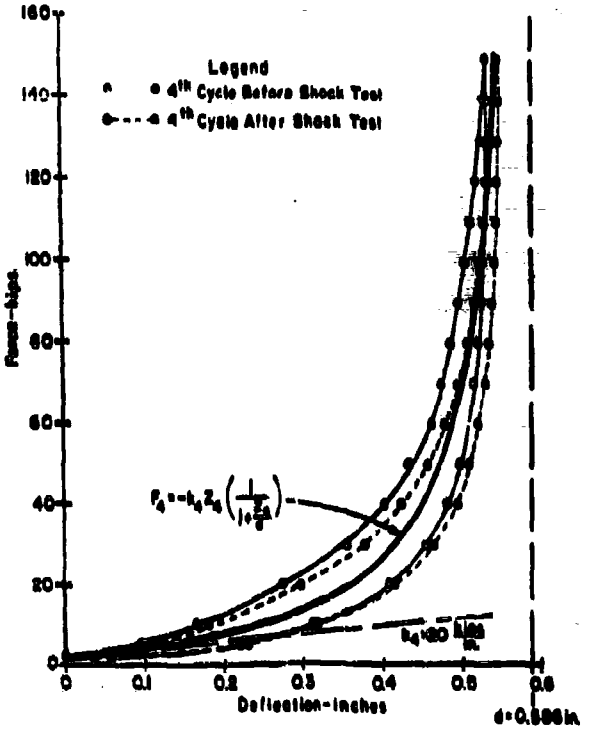

Figure 58 - Mathematical Nonlinear Characteristic Used for Spring K_4 Compared with Experimentally Measured Static Force-Deflection Curves

Other force relationships are as follows:

$$K_1 Z_1 = K_2 Z_2 + C_1 \dot{Z}_2 = -F_1$$

$$K_3 Z_3 = -F_4 + C_2 \dot{Z}_4 = -F_2.$$

The force F_3 can never become negative since the snubber cannot support tension. Therefore $F_3 \geq 0$.

Also	$Z_3 = Z - Z_4 + D_0$	for $Z_4 \geq Z + D_0$
but	$Z_3 = 0$	for $Z_4 \leq Z + D_0$.

The equation of motion of the mass M is, of course, $M\ddot{X} = F$.

The above equations are sufficient to describe the system given in Figure 57 and are those used as the basis for programming the computer. This entire system was considered to be at rest at time $t = 0$.

SYNTHESIS OF INPUT VELOCITY CURVES

Analysis of the experimental velocity measurements indicated that the input velocity versus time curves could be represented very well by assuming an instantaneous initial velocity with a constant average deceleration upon which a sinusoidal perturbation is superimposed. Such an equation is as follows:

$$\dot{X}_B = V_0 - At - B \sin \omega t$$

and differentiating,

$$\ddot{X}_B = u = A - \omega B \cos \omega t.$$

This equation is readily mechanized on the analog computer using a cosine waveform generated as follows:

let	$u = \sin \omega t$	and	$v = \cos \omega t$
and differentiating	$\dot{u} = \omega \cos \omega t$	and	$\dot{v} = -\omega \sin \omega t$
or	$\dot{u} = \omega v$	and	$\dot{v} = -\omega u$
where	$u_0 = 0$	and	$v_0 = 1$.

Numerical values for each of the coefficients in the above equations were selected to best fit the experimental measurements from each explosion test. These values are given in Table 9.

TABLE 9
Coefficients for Simulated Input Velocity Curves

Test No.	V_0 fps	A ft/sec^2	B fps	ω rad/sec
2	6.9	338	0.5	100 π
3	8.5	408	1.5	100 π
4	12	504	2.25	100 π
5	16	752	2.5	100 π

COMPUTER PROGRAMMING AND OPERATION

The computer used to obtain the solutions to this problem was a PACE, Model TR-48, manufactured by Electronic Associates, Incorporated. The equations were scaled, and the program was derived using the standard techniques, procedures, and diagrammatic symbols advocated by the manufacturer of this equipment. This program is presented in Figure 59. The potentiometer settings used for the final runs are given in Table 10.

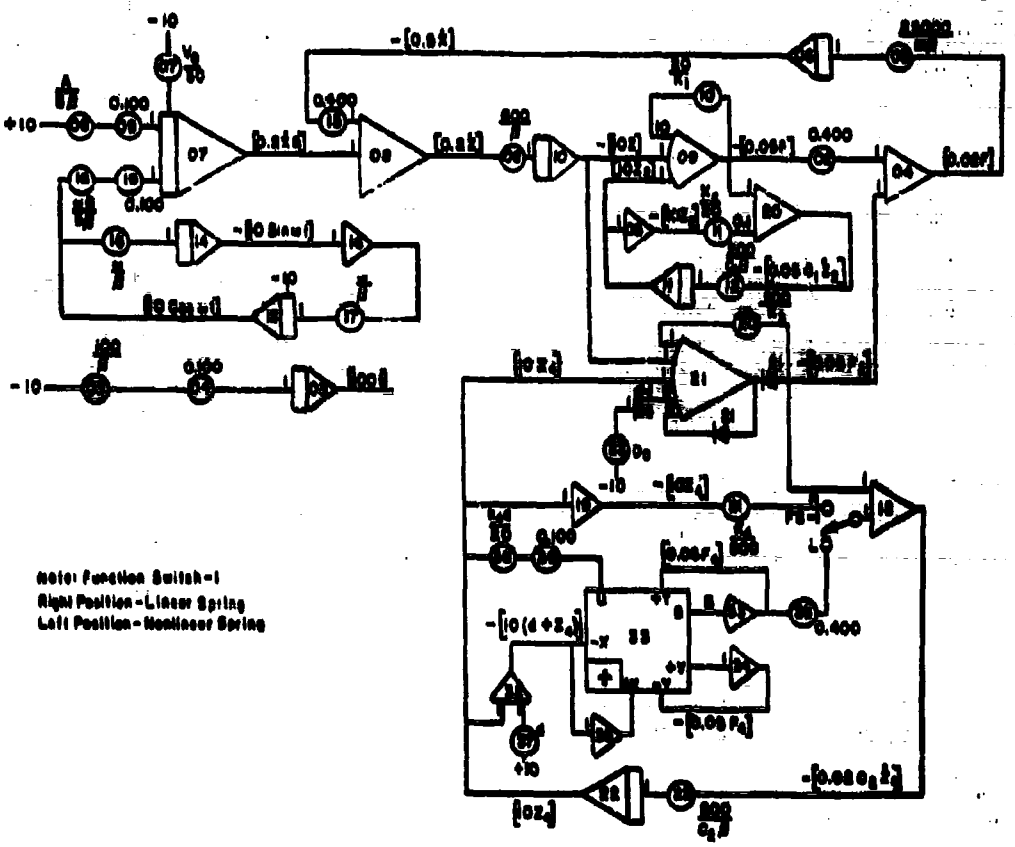

Figure 59 - Computer Program

In order to allow the computer solutions to be plotted on X-Y recorder, the time scale, β, was selected to be 1000; thus the problem was slowed by this factor.

The repetitive operation mode was used to determine the values of the system parameters. In this mode the computer automatically speeds the problem up by a factor of 500 and repetitively solves the problem at a rapid rate, displaying the results on a cathode ray oscilloscope. In this instance the total force (F) on the mass was displayed versus the relative displacement (Z) between the mass and the base.

TABLE 10
Computer Potentiometer Assignments

Potentiometer No.	Parameter Description	Potentiometer Setting for Computer			
		Run No. 1 (Test 4)	Run No. 2 (Test 5)	Run No. 3 (Test 3)	Run No. 4 (Test 2)
02	0.400	0.400	0.400	0.400	0.400
03	$100/\beta$	0.100	0.100	0.100	0.100
04	0.100*	0.100*	0.100*	0.100*	0.100*
05	$25000/K\beta$	0.101	0.101	0.101	0.101
06	$600/\beta$	0.600	0.600	0.600	0.600
07	$V_0/50$	0.240	0.320	0.170	0.130
08	$A/5\beta$	0.101	0.150	0.082	0.068
09	0.100*	0.100*	0.100*	0.100*	0.100*
10	$20/k_1$	0.308	0.308	0.308	0.308
11	$K_2/20$	0.150	0.150	0.150	0.150
12	$200/C_1\beta$	0.111	0.111	0.111	0.111
13	0.400	0.400	0.400	0.400	0.400
16	ω/β	0.314	0.314	0.314	0.314
17	ω/β	0.314	0.314	0.314	0.314
18	$\omega B/5\beta$	0.141	0.197	0.098	0.081
19	0.100*	0.100*	0.100*	0.100*	0.100*
20	$500/K_3$	0.660	0.660	0.660	0.660
21	$K_4/500$**	0.080**	0.080**	0.080**	0.080**
22	$500/C_2\beta$	0.106	0.106	0.106	0.106
23	D_0	0.312	0.312	0.312	0.312
35	0.400†	0.400†	0.400†	0.400†	0.400†
37	d	0.586	0.586	0.586	0.586
38	$k_4 d/20$	0.586	0.586	0.586	0.586
39	0.100*	0.100*	0.100*	0.100*	0.100*

* Set these potentiometers first to insure correct loading.
** Set with FS-1 "Right".
† Set with FS-1 "Left".

The various parameters of the system were then varied until this force versus deflection curve most nearly matched that derived from the particular explosion test being simulated. Once these parameter values had been established for one test, they were then used to determine the system response under other input conditions.

In addition to the force-deflection curves, amplitude versus time plots were obtained for four test conditions of the following variables:

a. Total force, F, on the mass

b. Relative deflection between the mass and the base

c. Absolute velocity, $\dot{X}$, of the mass

d. Absolute base velocity, $\dot{X}_B$.

INITIAL DISTRIBUTION

1 - 18	CHBUSHIPS
	1 - 3 Code 210L
	4 Code 320
	5 Code 341A
	6 - 10 Code 345
	11 - 12 Code 420
	13 - 15 Code 423
	16 - 18 Code 430
19	CO & DIR, USNMEL
20	CO & DIR, USNASL
21	CO & DIR, USNUSL
22	CO & DIR, USNEL
23	DIR, NRL (6260)
24	NAVSHIPYD MARE (Rubber Lab)
25 - 44	DDC

Special Project

UNCLASSIFIED

Security Classification

DOCUMENT CONTROL DATA - R&D

(Security classification of title, body of abstract and indexing annotation must be entered when the overall report is classified)

1. ORIGINATING ACTIVITY (Corporate author) David Taylor Model Basin Underwater Explosions Research Division Portsmouth, Va.	2a. REPORT SECURITY CLASSIFICATION Unclassified 2b. GROUP Not Applicable

3. REPORT TITLE

Response of 5M10,000-H Resilient Mounts under Shock Loading

4. DESCRIPTIVE NOTES (Type of report and inclusive dates)

5. AUTHOR(S) (Last name, first name, initial)

Thornton, Earl A., Short, Robert D., Jr., and Walker, Ramon R.

6. REPORT DATE	7a. TOTAL NO. OF PAGES	7b. NO. OF REFS
Jan 68	77	8

8a. CONTRACT OR GRANT NO. Special Project b. PROJECT NO. c. d.	9a. ORIGINATOR'S REPORT NUMBER(S) 1899 9b. OTHER REPORT NO(S) (Any other numbers that may be assigned this report)

10. AVAILABILITY/LIMITATION NOTICES

Foreign announcement and dissemination of this report by DDC is not authorized

11. SUPPLEMENTARY NOTES	12. SPONSORING MILITARY ACTIVITY

13. ABSTRACT

Experimental and theoretical studies of the type 5M10,000-H rubber resilient mount assembly consisting of a compression and shear mount and snubber were conducted to determine its performance under shock loading.

In the experimental study, the mount assembly (supporting a rigid test mass) was installed on the Floating Shock Platform and subjected to a series of five shock tests. The experimental data were analyzed and dynamic force-deflection curves were obtained.

Parallel theoretical studies were conducted. A simple mathematical model combining springs and dashpots was used to represent the response of the mounts under vertical shock loading. Theoretical dynamic force-deflection curves obtained from this system showed good agreement with the experimental data.

Findings of the experimental and theoretical studies led to the conclusion that dynamic force-deflection curves must be used in calculations of the shock response of supported equipment.

DD FORM 1 JAN 64 1473

UNCLASSIFIED

Security Classification

UNCLASSIFIED
Security Classification

14. KEY WORDS	LINK A		LINK B		LINK C	
	ROLE	WT	ROLE	WT	ROLE	WT
Vibration isolation						
Resilient mounts						
Shock waves						
Dynamic force-deflection curves						
Analog computer program						
Wave transmission, Elastic solid						
Rubber compression properties						
Impact vibrational aspects						
Mathematical analysis						
MIL-M-21649A (Ships), Military specification						
Experimental & Theoretical data						

INSTRUCTIONS

1. **ORIGINATING ACTIVITY:** Enter the name and address of the contractor, subcontractor, grantee, Department of Defense activity or other organization *(corporate author)* issuing the report.

2a. **REPORT SECURITY CLASSIFICATION:** Enter the overall security classification of the report. Indicate whether "Restricted Data" is included. Marking is to be in accordance with appropriate security regulations.

2b. **GROUP:** Automatic downgrading is specified in DoD Directive 5200.10 and Armed Forces Industrial Manual. Enter the group number. Also, when applicable, show that optional markings have been used for Group 3 and Group 4 as authorized.

3. **REPORT TITLE:** Enter the complete report title in all capital letters. Titles in all cases should be unclassified. If a meaningful title cannot be selected without classification, show title classification in all capitals in parenthesis immediately following the title.

4. **DESCRIPTIVE NOTES:** If appropriate, enter the type of report, e.g., interim, progress, summary, annual, or final. Give the inclusive dates when a specific reporting period is covered.

5. **AUTHOR(S):** Enter the name(s) of author(s) as shown on or in the report. Enter last name, first name, middle initial. If military, show rank and branch of service. The name of the principal author is an absolute minimum requirement.

6. **REPORT DATE:** Enter the date of the report as day, month, year; or month, year. If more than one date appears on the report, use date of publication.

7a. **TOTAL NUMBER OF PAGES:** The total page count should follow normal pagination procedures, i.e., enter the number of pages containing information.

7b. **NUMBER OF REFERENCES:** Enter the total number of references cited in the report.

8a. **CONTRACT OR GRANT NUMBER:** If appropriate, enter the applicable number of the contract or grant under which the report was written.

8b, 8c, & 8d. **PROJECT NUMBER:** Enter the appropriate military department identification, such as project number, subproject number, system numbers, task number, etc.

9a. **ORIGINATOR'S REPORT NUMBER(S):** Enter the official report number by which the document will be identified and controlled by the originating activity. This number must be unique to this report.

9b. **OTHER REPORT NUMBER(S):** If the report has been assigned any other report numbers *(either by the originator or by the sponsor)*, also enter this number(s).

10. **AVAILABILITY/LIMITATION NOTICES:** Enter any limitations on further dissemination of the report, other than those imposed by security classification, using standard statements such as:

(1) "Qualified requesters may obtain copies of this report from DDC."

(2) "Foreign announcement and dissemination of this report by DDC is not authorized."

(3) "U. S. Government agencies may obtain copies of this report directly from DDC. Other qualified DDC users shall request through _____."

(4) "U. S. military agencies may obtain copies of this report directly from DDC. Other qualified users shall request through _____."

(5) "All distribution of this report is controlled. Qualified DDC users shall request through _____."

If the report has been furnished to the Office of Technical Services, Department of Commerce, for sale to the public, indicate this fact and enter the price, if known.

11. **SUPPLEMENTARY NOTES:** Use for additional explanatory notes.

12. **SPONSORING MILITARY ACTIVITY:** Enter the name of the departmental project office or laboratory sponsoring *(paying for)* the research and development. Include address.

13. **ABSTRACT:** Enter an abstract giving a brief and factual summary of the document indicative of the report, even though it may also appear elsewhere in the body of the technical report. If additional space is required, a continuation sheet shall be attached.

It is highly desirable that the abstract of classified reports be unclassified. Each paragraph of the abstract shall end with an indication of the military security classification of the information in the paragraph, represented as *(TS), (S), (C), or (U)*.

There is no limitation on the length of the abstract. However, the suggested length is from 150 to 225 words.

14. **KEY WORDS:** Key words are technically meaningful terms or short phrases that characterize a report and may be used as index entries for cataloging the report. Key words must be selected so that no security classification is required. Identifiers, such as equipment model designation, trade name, military project code name, geographic location, may be used as key words but will be followed by an indication of technical context. The assignment of links, roles, and weights is optional.

DD FORM 1 JAN 64 1473 (BACK)

UNCLASSIFIED
Security Classification

David Taylor Model Basin. Report 1899
RESPONSE OF 5M10,000-H RESILIENT MOUNTS UNDER SHOCK LOADING, by Earl A. Thornton, Robert D. Short, Jr. and Ramon R. Walker. January 1965. vii, 70p. 59 figs., 10 tables, 8 refs. UNCLASSIFIED

Experimental and theoretical studies of the type 5M10,000-H rubber resilient mount assembly consisting of a compression and shear mount and snubber were conducted to determine its performance under shock loading.

In the experimental study, the mount assembly (supporting a rigid test mass) was installed on the Floating Shock Platform and subjected to a series of five shock tests. The experimental data were analyzed and dynamic force-deflection curves were obtained.

1. Rubber mounts - Response analysis
2. Vibration isolators-Response analysis
3. Impact vibration - Rubber mount response
4. Resilient mount specification - Dynamic & static force-deflection curves

I. Thornton, Earl A.
II. Short, Robert D., Jr.
III. Walker, Ramon R.
IV. Special Project

David Taylor Model Basin. Report 1899
RESPONSE OF 5M10,000-H RESILIENT MOUNTS UNDER SHOCK LOADING, by Earl A. Thornton, Robert D. Short, Jr. and Ramon R. Walker. January 1965. vii, 70p. 59 figs., 10 tables, 8 refs. UNCLASSIFIED

Experimental and theoretical studies of the type 5M10,000-H rubber resilient mount assembly consisting of a compression and shear mount and snubber were conducted to determine its performance under shock loading.

In the experimental study, the mount assembly (supporting a rigid test mass) was installed on the Floating Shock Platform and subjected to a series of five shock tests. The experimental data were analyzed and dynamic force-deflection curves were obtained.

1. Rubber mounts - Response analysis
2. Vibration isolators-Response analysis
3. Impact vibration - Rubber mount response
4. Resilient mount specification - Dynamic & static force-deflection curves

I. Thornton, Earl A.
II. Short, Robert D., Jr.
III. Walker, Ramon R.
IV. Special Project

David Taylor Model Basin. Report 1899
RESPONSE OF 5M10,000-H RESILIENT MOUNTS UNDER SHOCK LOADING, by Earl A. Thornton, Robert D. Short, Jr. and Ramon R. Walker. January 1965. vii, 70p. 59 figs., 10 tables, 8 refs. UNCLASSIFIED

Experimental and theoretical studies of the type 5M10,000-H rubber resilient mount assembly consisting of a compression and shear mount and snubber were conducted to determine its performance under shock loading.

In the experimental study, the mount assembly (supporting a rigid test mass) was installed on the Floating Shock Platform and subjected to a series of five shock tests. The experimental data were analyzed and dynamic force-deflection curves were obtained.

1. Rubber mounts - Response analysis
2. Vibration isolators-Response analysis
3. Impact vibration - Rubber mount response
4. Resilient mount specification - Dynamic & static force-deflection curves

I. Thornton, Earl A.
II. Short, Robert D., Jr.
III. Walker, Ramon R.
IV. Special Project

David Taylor Model Basin. Report 1899
RESPONSE OF 5M10,000-H RESILIENT MOUNTS UNDER SHOCK LOADING, by Earl A. Thornton, Robert D. Short, Jr. and Ramon R. Walker. January 1965. vii, 70p. 59 figs., 10 tables, 8 refs. UNCLASSIFIED

Experimental and theoretical studies of the type 5M10,000-H rubber resilient mount assembly consisting of a compression and shear mount and snubber were conducted to determine its performance under shock loading.

In the experimental study, the mount assembly (supporting a rigid test mass) was installed on the Floating Shock Platform and subjected to a series of five shock tests. The experimental data were analyzed and dynamic force-deflection curves were obtained.

1. Rubber mounts - Response analysis
2. Vibration isolators-Response analysis
3. Impact vibration - Rubber mount response
4. Resilient mount specification - Dynamic & static force-deflection curves

I. Thornton, Earl A.
II. Short, Robert D., Jr.
III. Walker, Ramon R.
IV. Special Project

Parallel theoretical studies were conducted. A simple mathematical model combining springs and dashpots was used to represent the response of the mounts under vertical shock loading. Theoretical dynamic force-deflection curves obtained from this system showed good agreement with the experimental data.

Findings of the experimental and theoretical studies led to the conclusion that dynamic force-deflection curves must be used in calculations of the shock response of supported equipment.

Parallel theoretical studies were conducted. A simple mathematical model combining springs and dashpots was used to represent the response of the mounts under vertical shock loading. Theoretical dynamic force-deflection curves obtained from this system showed good agreement with the experimental data.

Findings of the experimental and theoretical studies led to the conclusion that dynamic force-deflection curves must be used in calculations of the shock response of supported equipment.

Parallel theoretical studies were conducted. A simple mathematical model combining springs and dashpots was used to represent the response of the mounts under vertical shock loading. Theoretical dynamic force-deflection curves obtained from this system showed good agreement with the experimental data.

Findings of the experimental and theoretical studies led to the conclusion that dynamic force-deflection curves must be used in calculations of the shock response of supported equipment.

Parallel theoretical studies were conducted. A simple mathematical model combining springs and dashpots was used to represent the response of the mounts under vertical shock loading. Theoretical dynamic force-deflection curves obtained from this system showed good agreement with the experimental data.

Findings of the experimental and theoretical studies led to the conclusion that dynamic force-deflection curves must be used in calculations of the shock response of supported equipment.